LUND UNIVERSITY

Mircostructure and rheological properties of concentrated tomato suspensions during processing

Bayod, Elena

2008

Microstructural and Rheological Properties of Concentrated Tomato Suspensions during Processing

Elena Bayod

2008

Doctoral thesis

Division of Food Engineering

Department of Food Technology, Engineering and Nutrition

Lund University

Microstructural and Rheological Properties of Concentrated Tomato Suspensions during Processing

A doctoral thesis at a university in Sweden is produced either as a monograph or as a collection of papers. In the latter case, the introductory part constitutes the formal thesis, which summarizes the accompanying papers. These have either already been published or are manuscripts at various stages (in press, submitted or in ms).

Cover: micrographs of tomato suspensions at different stages of processing

Abstract

Food processing comprises operations such as dilution (changing the concentration), homogenisation (changing the particle size), and subsequent pumping (shearing), among others. It is thus of great interest to gain a better understanding of the mechanisms governing the creation and disruption of structures during these engineering operations, and the way in which they are related to the textural and rheological properties of the material.

The influence of processing on the microstructure and the rheological properties of tomato paste suspensions has been studied. The microstructure was characterised using light microscopy and particle size distribution analysis. The way in which particles of varying size are packed in a specified volume at different concentrations was estimated in terms of the compressive volume fraction. The rheological properties were studied using small-amplitude oscillatory tests, giving the elastic (G') and viscous (G'') moduli, as well as steady shear measurements, giving the viscosity (η). In the latter case both a rotational and a tube viscometer were used.

The results indicate that tomato suspensions consist of a collection of whole cells and cell wall material forming a network ($G'>G''$). During the process of homogenisation, the particles are broken down, resulting in a smoother and more evenly distributed network of finer particles. The effectiveness of homogenisation in decreasing particle size seemed to be governed by the inherent susceptibility of the particles to breakage (i.e. the type of paste), the viscosity of the suspending medium, and the concentration of particles. Higher viscosities and concentrations were found to prevent breakage to some extent.

The presence of larger amounts of fine particles in the homogenised suspensions had a considerable effect on the rheological properties. The yield stress was found to increase, and time-dependent effects became more apparent. At low deformations ($\gamma \leq 20$), the system consisting of finer particles exhibited rheopectic behaviour (increasing viscosity with time), which was suggested to be caused partly by the rotation of the particles

induced by the flow, and partly by the remaining elastic behaviour at stresses close to the yield stress. At larger deformations ($\gamma \leq 1000$), the non-homogenised system exhibited steady-state viscosity, while in the homogenised system it continued to decrease. The unstable behaviour observed in homogenised systems at large deformations gave an indication of particle rearrangement under flow conditions. Micrographs of homogenised suspensions subjected to shearing showed the formation of flocs consisting of densely packed particles that could easily orient in the shearing direction. At high concentrations, the changes in the microstructure caused by homogenisation and shearing were better reflected by the compressive volume fraction than by the elastic modulus.

Tube viscometer measurements showed the presence of wall slip in highly concentrated tomato suspensions, which tended to disappear at lower concentrations. The wall slip, which could be as high as 70% of the flow rate, was estimated using both the classical Mooney approach and an inverse numerical method, and the performance of these two methods was compared. The performance of the methods was complicated by the relatively poor reproducibility of the data. Steady shear rheological measurements obtained using a rotational rheometer with different geometries (concentric cylinders, vane, vane-vane) and tube viscometer measurements agreed when no slip was present, and the vane and vane-vane geometries were found to be free of wall slip effects.

Finally, the applicability of the Cox-Merz rule (superposition of oscillatory and steady shear data) seemed to be limited to systems that do not form a network ($G'<G''$), and did not apply to structured systems having a yield value and $G'>G''$. However, the dynamic and steady shear data obtained for tomato suspensions coincided when using a shifting factor of about 0.1 on the frequency , which was fairly constant for a large range of tomato paste concentrations (from 100 to 30%, all with $G'>G''$).

Populärvetenskaplig sammanfattning

Världens produktion av tomat har ökat kraftigt under de senaste årtiondena och 2004 översteg den 100 miljoner ton. Tomat brukar konsumeras huvudsakligen som färsk grönsak och/eller som processad tomatprodukt. Tomatpasta är den huvudprodukt, som används vid tillverkning av tomatketchup och tomatsås. I Sverige, är ketchupkonsumtionen omkring 2 kg per person och år, och försäljningen uppgår till mer än 330 MSEK. Tomatketchup består av tomatpasta, vatten, socker, vinäger, salt, kryddor, och ibland också lök och vitlök som smaktillsats. Även andra tillsatser, såsom förtjocknings- och stabiliseringsmedel, kan användas för att påverka konsistensen. Smak och textur/konsistens är för konsumenter de viktigaste parametrarna för att bedöma kvaliteten hos ketchup. Man vill ha en produkt som smakar gott, men konsistensen måste vara sådan så att man får rätt munkänsla. Det är också viktigt att undvika ketchupeffekten, dvs. först kommer inget och sen kommer allt på en gång. Andra kvalitetsaspekter avseende konsistensen är att tomatketchupen skall ligga kvar på korven när man äter den. En kvalitetsdefekt hos ketchup, som kan uppfattas negativt av konsumenten, är serumseparation, som uppkommer som ett tunt vätskeskikt ovanför ketchupen vid flaskhalsen. Det är därför viktigt att förstå hur tillverkningsprocessen påverkar konsistensen hos ketchup för att förbättra kvaliteten och minska olika kvalitetsdefekter. Syftet med denna studie var att lära sig mer om hur tomatfibrerna uppträder under olika processer, som används för att tillverka såser eller ketchup, och att studera de mikrostrukturer som kan uppkomma under denna processning. Exempel på sådana processer är homogenisering och pumpning.

Tomatprodukter kan beskrivas som ett disperst system, där den fasta fasen utgöres av tomatceller och delar av tomatcellen i form av fibrer och dessa är uppslammade i vatten med socker och andra lösliga ämnen. Vid processning av detta system förändras produktens struktur och mekaniska egenskaper, vilket ger upphov till olika textur och konsistens. Ett sätt att förutsäga dessa olika konsistenser är att mäta produkternas mikrostruktur och reologiska egenskaper. Reologin är den vetenskap som behandlar flyt- och deformationsegenskaper. I föreliggande arbete har effekten av processning

(homogenisering och pumpning) undersökts med avseende på olika utspädda tomatpastors mikrostruktur och reologi. Homogenisering ger mindre partikelstorlek och förbättrar viskositeten (konsistensen), medan produkterna är efter denna behandling mer känsliga för fiberaggregering vid efterföljande pumpning. Denna mikrostrukturella förändring kan ge oönskad lägre viskositet och serumseparation.

Pumpning är en viktig och oundviklig del vid tillverkning av exempelvis tomatketchup, och för att beräkna pumpens prestationsförmåga krävs bland annat att man känner till tomatketchupens viskositet. Att överdimensionera pumpen i processen är både ekonomiskt och energetiskt dyrt, men att underdimensionera pumpen kan orsaka allvarliga problem för livsmedelsindustrin om livsmedlet ifråga inte kan pumpas vidare. Därför är det intressant att mäta viskositeten noggrant. Olika problem kan förekomma vid mätning av viskositet hos produkter med högt fiberinnehåll, som tomatpasta. Exempelvis, uppträder vid väggen av mätinstrumentet ett väldigt tunt skikt av vätska på grund av partikelrörelse bort från väggen. Detta fenomen kallas slip. Det gör att man mäter en lägre viskositet än det i verkligheten är och dimensionerar därför pumpen fel utifrån den för låga viskositeten. Att kontrollera och korrigera för denna slip så att viskositetsmätningarna blir korrekta har också varit en del av detta arbete.

Denna studie är ett samarbete med Orkla Foods AS, Tetra Pak AB, Lyckeby-Culinar AB, Reologica AB, Salico, AB, Mariannes Farm AB, Kiviks Musteri AB.

List of Papers

This thesis is based on the following papers, which will be referred to in the text by their Roman numerals. The papers are appended at the end of the thesis.

Paper I.   Bayod E., Willers, E. P., Tornberg E. (2007)
Rheological and structural characterization of tomato paste and its influence on the quality of ketchup
LWT - Food Science and Technology, In Press, DOI: 10.1016/j.lwt.2007.08.011

Paper II.   Bayod E., Månsson P., Innings F., Bergenståhl B., Tornberg E. (2007)
Low shear rheology of tomato products. Effect of particle size and time
Food Biophysics, 2 (4), 146-157

Paper III.   Bayod E., Tornberg E. (2008)
Microstructure of highly concentrated tomato suspensions during homogenisation and after subsequent shearing
Submitted for publication, 2007

Paper IV.   Bayod E., Jansson P., Innings F., Dejmek P., Bolmstedt U., Tornberg E. (2008)
Rheological behaviour of concentrated fibre suspensions in tube and rotational viscometers, in the presence of wall slip.
Manuscript

Author's contribution to the papers

Papers I and III. The author designed the experiment based on discussions with the co-authors. The author performed all the experimental work, evaluated the results and wrote the papers.

Paper II. The author designed the experiment based on discussions with the co-authors (FI, BB, ET) and performed part of the experimental work together with PM. The author evaluated the results and wrote the paper.

Paper IV. The author designed the experiment based on discussions with the co-authors (PJ, FI, UB, ET) and performed part of the experimental work together with PJ. The author wrote the Matlab code together with PD. The author evaluated the results and wrote the paper.

Related publications

Bayod E., Bergenstahl B., Innings F., Tornberg E. **(2008)**. The susceptibility to create shear induced flocs in tomato fiber suspensions on homogenisation and shearing. *Accepted for presentation at the 10th International Congress of Engineering and Food*, Viña del Mar, Chile, April 20-24, 2008.

Bayod E., Tornberg E. **(2008)**. Insights into the microstructural properties of tomato products. *Accepted for presentation at Food Colloids,* Le Mans, France, April 6-9, 2008

Bayod E., Månsson P., Innings F., Bergenståhl B., Tornberg E. **(2006).** Combined effect of both stress and time on the viscosity of high concentrate fibre suspensions. *Proceedings of the 4th International Symposium on Food Rheology and Structure*, pp. 523-527, Zurich, Switzerland

Bayod, E., Bolmstedt, U., Innings, F., Tornberg, E. **(2005)**. Rheological characterization of fiber suspensions prepared from vegetable pulps and dried fibers. A comparative study. *Proceedings of the Nordic Rheology Conference*, pp. 249-253, Tampere, Finland

Abbreviations and Symbols

		Symbols			**Greek letters**
a_p	-	Aspect ratio	α	-	Slip behaviour index
d_{32}	μm	Area-based diameter	β	m/Pa$^\alpha$ s	Slip coefficient
d_{43}	μm	Volume-based diameter	γ	-	Strain/deformation
D_f	-	Fractal number	$\dot{\gamma}$	1/s	Shear rate
d	-	Euclidian space dimension	η	Pa s	Apparent viscosity
d_i	m	Inner tube diameter	η^*	Pa s	Complex viscosity
d_o	m	Outer tube diameter	η_0	Pa s	Zero-shear viscosity
dP	Pa	Pressure drop	η_s	Pa s	Viscosity of the supernatant
E	J	Energy	θ	º	Angle of rotation
f/c	-	Fine-to-coarse particle ratio	λ	s	Time constant, Carreau
G*	Pa	Complex modulus	μ	Pa s	Newtonian viscosity
G'	Pa	Elastic/storage modulus	N	-	Exponent, Carreau
G"	Pa	Viscous/loss modulus	σ	Pa	Shear stress
h	m	Vane height	σ_w	Pa	Wall shear stress
k	J/K	Boltzman constant	σ_y	Pa	Yield stress
K	Pa s^n	Consistency coefficient	ϕ	-	Volume fraction
L	m	Length	ϕ_m	-	Maximum packing fraction
M	N m	Torque	ϕ_c	-	Critical concentration fraction
n	-	Flow behaviour index	Ω	rad/s	Angular velocity
N_j, N_k	-	Number of points j, k	ω	Hz	Frequency
Q	m³/s	Flow rate			
Q_m	m³/s	Measured flow rate			
Q_s	m³/s	Flow rate due to slip			
Q_{ws}	m³/s	Flow rate without slip			
R	m	Inner tube radius			
Re	-	Reynolds number			
R_i	m	Bob radius			
R_o	m	Cup radius			
S_1	-	Tikhonov error			
S_2	-	Tikhonov smoothness			
t	s	Time			
v_s	m/s	Slip velocity			
v_x	m/s	Velocity along x-axis			
v_θ	m/s	Velocity in θ			

Abbreviations

ah		After homogenisation
bh		Before homogenisation
CB		Cold break
CC		Concentric cylinder
EDM		Euclidean distance map
H		Homogenisation
HB		Hot break
LVE		Linear viscoelastic region
PSD		Particle size distribution
SH		Shearing
TS	%	Total solids
V		Vane geometry
VV		Vane geometry in vane cup
WIS	%	Water-insoluble solids

Contents

1. Introduction

Tomatoes are an important commercial product, with a total world production in 2004 exceeding 100 million tones (UN Food and Agricultural Organization). Tomatoes can be consumed fresh, although most of the global production is processed to form tomato paste. This tomato paste is then used as a main ingredient in other products such as ketchup, sauces, and juices. The principal quality parameters for consumer acceptance of tomato products are the appearance, colour and flavour, as well as the consistency and texture, which in turn depend on the agronomical conditions during the growth of the tomatoes and the processing conditions during the production of different tomato products.

Processing fresh tomatoes to provide tomato paste involves a number of stages. First, the fresh tomatoes are washed, sorted and crushed, usually accompanied by thermal treatment (called break treatment), followed by peeling, screening and refining. The fluid is then concentrated by evaporation, finally undergoes thermal treatment (pasteurisation/sterilization) and packaging, often aseptic vacuum-packing. The viscosity increases throughout the concentration processes, from about 10 mPa s in the initial tomato juice up to viscosities several orders of magnitude higher in the final tomato paste. The final product should be as concentrated as possible (usually between 24 and 38% soluble solids), but it should still be pumpable to allow processing. This means that the accurate determination of the pumping requirements is of great interest. Predictions of the pressure drop in tomato paste in tube flow based on viscosity values obtained from rotational rheometers, are frequently found to be incorrect, according to manufacturers' experience, but no investigation has so far addressed this problem. It has been observed in concentrated tomato products that substantial wall slip occurs on tube flow (Lee et al., 2002) and this may be a reason for the disagreement between tube and rheometer viscosity data.

The method of producing tomato paste influences the quality of the products to which it is added as an ingredient, for example, ketchup. The process parameters believed to have

the greatest effects on the rheology of tomato derivatives are the break temperature, and the screen size (Valencia et al., 2004). Break treatment can be carried out at high temperatures (> 85°C), i.e. hot break (HB), or at low temperatures (< 70°C), i.e. cold break (CB). The latter process allows a certain degree of pectin degradation because of the slow and incomplete inactivation of the enzymes involved, i.e. pectin methyl esterase and polygalacturonase. This results in products with a lower viscosity, but better preserves the tomato flavour and colour. The influence of the break temperature on the rheological properties of tomato products has been studied previously (Fito et al., 1983; Xu et al., 1986). Moreover, changes in the pectin content and composition during the processing of HB tomato paste have been described (Hurtado et al, 2002). The difference in the physical properties of soluble pectin in HB and CB tomato paste has been attributed to lower average molecular mass and a different chemical structure in the latter case (Lin et al., 2005). It is believed that a higher pectin content gives rise to higher viscosity and better textural properties, but Den Ouden (1995) showed that the contribution of the pectins to the total viscosity was very small, compared with the contribution of the fibre matrix. The effect of the particle size has also been studied to some extent (Valencia et al. 2004, Den Ouden, 1995), but the published data are ambiguous.

Tomato products can be manufactured by diluting tomato paste to the desired content, mixing with other ingredients (i.e. spices, salt, sugar, vinegar, hydrocolloids), in some cases homogenisation, and then pasteurization, aseptic cooling and packing. Homogenisation is performed to obtain a smoother texture, enhance the structure of the product, to increase its viscosity and to lower the degree of syneresis (Thakur et al., 1995; Den Ouden, 1995). Generally, tomato products are non-Newtonian, shear thinning fluids that exhibit yield stress and are strongly dependent on the shear history of the fluid. For example, tomato juice has been shown to exhibit rheopectic behaviour at low deformations (De Kee, 1983), i.e. the viscosity increases as a function of time, and thixotropic behaviour at large deformations, i.e. the viscosity decreases as a function of time (Tiziani & Vodovotz, 2005). The latter has been suggested to be caused by structural breakdown of the suspension. This behaviour reflects the complex rheological nature of tomato products. Tomato products are considered to be concentrated food suspensions, consisting of whole cells or cell wall material suspended in an aqueous solution containing sugars, soluble pectins and proteins.

2. Scope

Tomato processing constitutes an important industry as large volumes of fresh tomatoes are processed into tomato ketchup and other products all over the world. As tomato products are consumed worldwide, understanding the influence of processing on their quality is of great interest, for both industry and consumers. Because of their economic impact, tomato products have been subjected to numerous investigations, usually involving their rheological characterisation. The complex nature of tomato suspensions can complicate rheological measurements in several ways and thus, the results obtained depend on the experimental conditions. A better understanding of the difficulties encountered in rheological measurements might allow us to correct for them and/or to prevent them, as well as providing more knowledge on tomato suspensions. Moreover, the influence of the tomato fibres and the microstructure of the suspensions on their textural and rheological attributes have been little explored so far.

The objectives of this investigation were therefore:

- To study the different problems encountered in the determination of the rheological properties of highly concentrated suspensions, such as tomato products. The determination of the yield stress, and the effect of time dependency and shear history are reported in **Paper II**, and the determination of the wall slip in both tube viscometers and rotational rheometers is described in **Paper IV**.

- To study the effect of processing on the properties of tomato products. The influence of homogenisation on the particle size distribution (PSD) and particle shape, and the effect of the PSD on the rheological properties of the suspensions, regarding the flow behaviour (**Paper I**), and the time dependency and yield stress (**Paper II**) have been investigated. Changes in the microstructure of the suspensions resulting from processing, i.e. homogenisation and shearing, have also been investigated (**Paper III)**.

3. The Microstructure of Food Suspensions

The processing of foods brings about several changes in their microstructure. The macroscopic properties of foods, such as rheology and mechanical strength, sensory attributes, as well as engineering properties, are strongly determined by the microstructure of the food material (Fig. 1). During the early development of the food industry, food engineers were mainly concerned with the macroscopic scale, which meant designing equipment and improving unit operations. Food manufactures were essentially concerned with producing large quantities of food of more or less acceptable quality. Nowadays, higher food quality is an increasing consumer demand, together with the development of new products. Because several sensory attributes, e.g. mouth feel, texture and even flavour release, are directly related to the microstructure and mechanics of food materials, understanding the effect of microstructure on the macroscopic properties of foods is a new challenge facing food researchers.
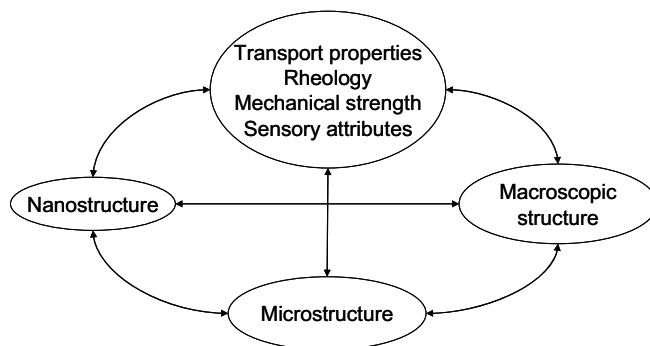
Figure 1. Schematic showing the hierarchy of food structure.

In 1980, Raeuber and Nikolaus noted the importance of food structure and its relation to textural and rheological properties. They recognised food materials consisting of elements at different structural levels, from the nanostructure (molecular level), to the macroscopic level (animal or vegetable tissues). They pointed out the importance of both the shape and arrangement of the primary elements on the mechanical properties of the material and, hence only by combining the microstructure with the mechanical behaviour

is it possible to obtain a complete picture of a material's properties. However, the research in this area has been relatively scarce and, as late as 2005, Aguilera (2005) wrote a paper entitled "Why Food Microstructure?" in which he highlights the importance of understanding food microstructure in both food process engineering and food design.

3.1 Observation of the microstructure

Processing can drastically change the mechanical properties, as well as the microstructure, of food products. An important example is that of whole fruits that are crushed to produce purees or juices; where both the whole fruit and the juice have approximately the same chemical composition, but their textural attributes are completely different. The process of high pressure homogenisation is another example of a process causing drastic changes in the microstructure, but on the microscopic scale (Fig. 2). Understanding the macroscopic properties governing food systems with similar composition, such as tomato suspensions before and after homogenisation, as shown in Figure 2, thus involves the characterisation and quantification of their microstructure.
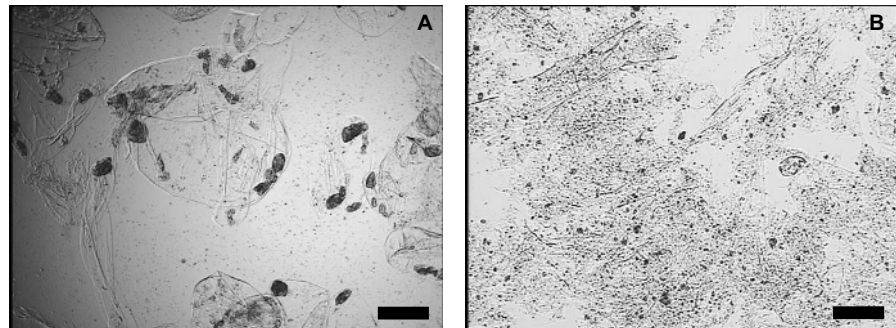
Figure 2. Typical micrograph of A) tomato cells and B) tomato cell fragments after homogenisation. The scale bar is 150 μm. (Adapted from **Paper I**.)

Microscopy is the most direct way of examining the microstructure of food materials, and provides valuable information on the shape and arrangement of the particles in diluted and semi-diluted systems. However, this type of observation can only be made on diluted systems, and it is often not suitable for highly concentrated food suspensions, which are dense, frequently opaque, and contain large particles (10-1000 μm). Diluting

highly concentrated suspensions to a concentration suitable for observation in a light microscope will, however, have a considerable effect on the structure of the suspension and the arrangement of the particles, so the structure observed will not resemble the original microstructure. Static light scattering is another technique that fails in systems subject to strong multiple scattering, such as concentrated food suspensions. Confocal microscopy is the preferred technique in such cases, but it requires some kind of fluorescent labelling of the structure under study and, in vegetable material, problems such as auto-fluorescence are likely to occur. Other techniques used in characterising food microstructure are summarised and their applicability and limitations discussed elsewhere (Wyss et al., 2005).

3.1.1   Morphology and shape of particles

The morphology of vegetable cells differs depending on the kind of tissue and its function in the living vegetable. Different types of cells also show different mechanical and textural properties. The different types of cells encountered in processed fruit products, such as tomato paste, are (Fig. 3): parenchyma cells, lignified skin cells, vascular tissue (e.g. xylem cells) and parts of the seeds. Parenchyma cells constitute the major fraction of the cells present in tomato paste, and they are characterised by their high deformability, low mass density and large volume fraction (Table 1). The aggregates of skin cells, vascular bundles and xylem are harder, high-density materials, and less deformable (Ilker & Szczesniak, 1990). Products enriched with the latter type of cells have lower viscosities and lower yield stresses (Den Ouden & Van Vliet, 1997).

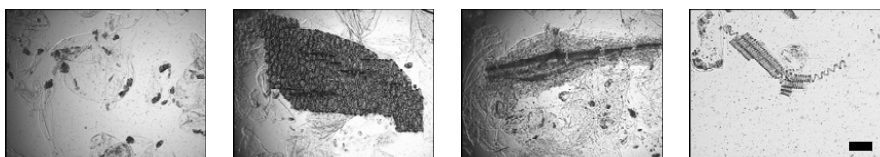Figure 3. Examples of different kinds of cells and cellular structures present in the tomato pastes studied in this work. From left to right: parenchyma cells, skin cells, vascular tissue and xylem cell. The scale bar is 150 µm .

Parenchyma cells are almost spherical and can be assumed to behave as spherical particles at rest, although they are highly deformable. Den Ouden and Van Vliet (1997)

found that tomato cells can pass through the pores of a sieve significantly smaller than the size of the cell itself. The aspect ratio, a_p, of the parenchyma cells, i.e. the relation between the length and width of the particles, is normally close to 1. The other types of cells are found in very small proportions in tomato paste, and have irregular shapes and variable aspect ratios (Fig. 3).

Table 1. Types of cells present in tomato paste, and the typical mechanical properties. Adapted from Den Ouden and Van Vliet (1997).

Cell type	Size	Deformability	Density	Properties
Parenchyma cells	<250 μm	Highly deformable	Low mass density Large volume fraction	High viscosity and yield stress
Aggregates of cells from skin, seeds and vascular bundles	> 250 μm	Less deformable	High mass density Low volume fraction	Low viscosity and yield stress

The shape and morphology of the particles in tomato products are drastically changed after homogenisation (Fig. 2B). The majority of the cells are broken down into smaller particles, resulting in a system containing large numbers of small particles such as fibre particles, cell and cell wall fragments, pectins and other polymers. The new arrangement of the particles in the suspension creates a more continuous and homogeneous system, giving rise to a different type of network structure.

3.2 Quantifying the microstructure

One of the reasons for the delay in incorporating microstructure into mechanical models in materials science is the difficulty in quantifying it. The human capacity to quantify visual features is limited by our own vision, and it is difficult to make objective assessments. The development of computers and new image analysis techniques has provided new means of quantifying images. A good description of the available image processing techniques can be found in the handbook by Russ (2007).

Other ways of "measuring" microstructure by more indirect techniques may be useful in concentrated suspensions where direct observation is difficult, since the mechanical

behaviour of a suspension or gel depends to a great extent on the volume fraction, the size and shape of the particles, the interparticle forces and the spatial arrangement between particles (Wyss et al., 2005), all contributing to what is termed the microstructure.

3.2.1   Image analysis of light micrographs

In the light micrograph images described in **Paper III**, image processing was necessary to correct for uneven illumination. This is a common problem in microscopic images, and can be seen, for example, in Figure 4A, where the right side of the image is much darker than the left side The differences in illumination were corrected using the rolling ball technique (radius=40 pixels). Image analysis is commonly performed on binary images, obtained by thresholding. In order to reduce the noise in the image a mean filter (radius=1.5 pixels) was first applied, and thresholding was automatically performed at a fixed grey intensity value of T=137, providing the binary images (Fig. 4B, 5B). Some simple analysis can be performed on binary images, for example, measurements of the area occupied by particles (i.e. the sum of the black pixels) and calculation of the fractal number associated with the image, using a box counting procedure.
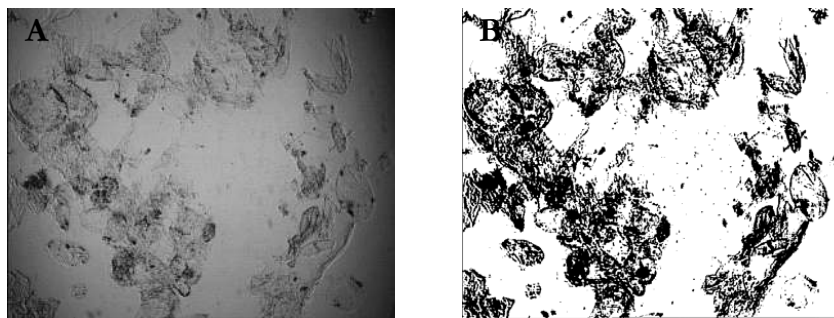
Figure 4. Micrograph showing uneven illumination (A) and binary image after correction (B).

It is also of interest to measure the distance between the particles and/or the size of the pores in the images. For this purpose, the binary image shown in Figure 5B was subjected to a series of closing, opening, dilate and erode operations to identify the particles and separate them from the background **(Paper III)** (Fig. 5C). Since we are interested in the voids in this image, it is necessary to invert the processed image (Fig.

5D). Combining a so-called Euclidean distance map (EDM, Fig. 5E), in which the distance between black points is expressed as grey values, and the skeleton of the voids, which represents the maximum distance between two points, allows us to gain information about the distance between two particles at several points. The reference points for the distance measurements correspond to the branching in the skeleton. These points are obtained by eroding points of the skeleton that have 6 or more background neighbours. In Figure 5F, the original picture, the skeleton of the voids and the reference points are combined.
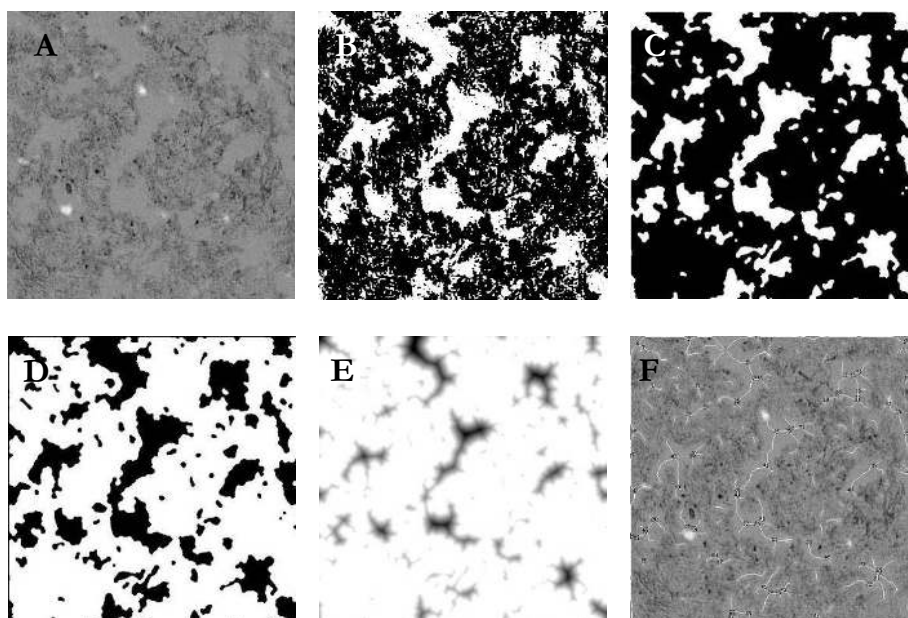
Figure 5. Examples of the results of image processing of the micrographs presented in **Paper III**. Image after defect correction (A), threshold image (B), image after binary operations (C), inverse binary image (D), distance map (E), and combined images original + skeleton (white line) + "reference" points (white line intersections) (F).

3.2.2   Particle size distribution

The particle size distribution (PSD) of food suspensions has a considerable influence on the rheological properties. The size distribution of particles can be determined using different techniques, for example, wet sieving, light microscopy and laser light diffraction. The last technique has been widely used throughout these studies, and the

diffraction data were analysed using the Fraunhofer diffraction method. The Fraunhofer method can be applied to particle sizes between 1 and 200 μm (Annapragada & Adjei, 1996), and can handle polydisperse systems. It assumes that the particles are spherical, but it adequately describes the particle size of fibres (i.e. cylinders) with diameters larger than 8 μm (Powers & Somerford, 1978). The use of the Fraunhofer theory in determining the PSD of tomato products is rather common (Den Ouden & Van Vliet, 1997; Getchell & Schlimme, 1985).

The size of the particles is usually expressed as the equivalent spherical diameter, and can be calculated based on the volume or the area occupied by the particles, d_{43} and d_{32}, respectively,

$$d_{43} = \sum_i n_i d_i^4 \bigg/ \sum_i n_i d_i^3 \qquad (1)$$

$$d_{32} = \sum_i n_i d_i^3 \bigg/ \sum_i n_i d_i^2 \qquad (2)$$

where n_i is the percentage of particles with diameter d_i. The volume-based diameter is mainly determined by the large particles present in the suspension. The area-based diameter also takes smaller particles into account. Small particles are important in determining the textural properties of the material, because they occupy the space between the larger particles and contribute to the network structure of the suspension. Moreover, a qualitative comparison between d_{32} and microscope images of tomato suspensions gives considerably better agreement than that using d_{43} (ocular observations from results presented in **Paper II**).
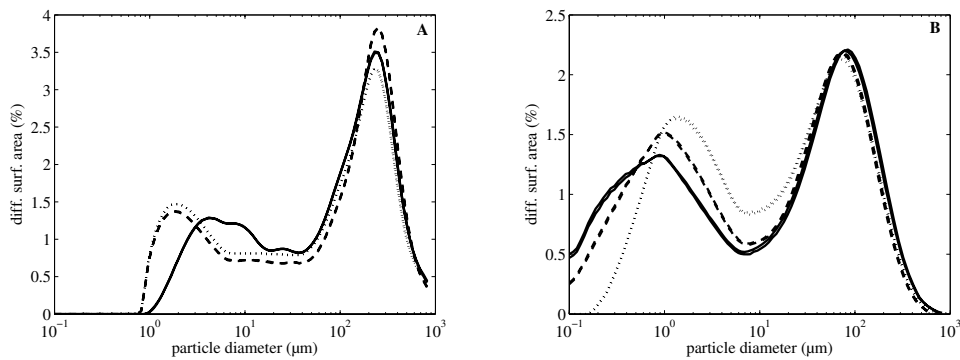

Figure 6. Particle size distribution of three tomato pastes (A) and the corresponding processed ketchups (B), expressed as the percentage surface area (%) as a function of the particle diameter (μm) (**Paper I**).

Particle size distributions are often expressed as the percentage of particles found in each size class (as in Figure 6). Foodstuffs often consist of polydispersed particles, with continuous particle size distributions containing several peaks, i.e. particles of all sizes are present, but most of them are of one or two specific. In tomato products, the PSD expressed in terms of the area-based diameter is usually considered to be bi-modal, i.e. consisting essentially of particles with two sizes (Fig. 6), and better describes the changes in the suspensions during processing than the volume-based diameter (d_{43}). **Papers I, II** and **III** describe the changes in the size of the particles due to homogenisation. The percentage of coarse particles (>10 μm) and fine particles (<10 μm), and the average size of each fraction are summarized in Table 2, for tomato suspensions before homogenisation, and after homogenisation to the particle size found in commercial ketchup. Based on the results given in **Paper I**, it is suggested that different HB pastes have different susceptibilities to breakage during homogenisation, depending on the viscosity of the supernatant.

Table 2. Morphological properties of the tomato pastes studied based on their area-based PSDs **(Papers I-III)**. The percentage of fine (< 10 μm) and coarse (> 10 μm) particles present in the suspensions, and the median diameters of the two fractions, before and after homogenisation to the particle size found in ketchup are given.

		Paper I			Paper II			Paper III
Paste type[a]		HB 28/30	HB 28/30	HB 28/30	HB 28/30	HB 22/24	CB 36/38	CB 36/38
Before homogenisation								
Coarse fraction	%	76	72	69	73	76	63	73
d_{32}	μm	170	196	169	202	157	123	177
Fine fraction	%	24	28	31	27	24	37	27
d_{32}	μm	4.4	2.7	2.7	2.5	3.5	3.1	3.1
After homogenisation								
Coarse fraction	%	53	51	54	59	53	41	38
d_{32}	μm	85	78	82	62	64	81	63
Fine fraction	%	47	49	46	41	47	59	62
d_{32}	μm	2.7	2.1	2.1	2.6	2.5	0.6	0.5

[a] 28/30 are the concentration of soluble solids expressed in ºBrix

The PSD can also be presented by plotting the cumulative percentage of particles as a function of the particle diameter, as in Figure 7. This way of expressing the particle size distribution facilitates the mathematical treatment and better reflects the changes caused

by small changes in processing, for example, varying the degree of homogenisation slightly. Suspensions of different concentrations were subjected to different number of passages through the homogeniser in order to obtain a final particle size similar to that of commercial ketchup **(Paper II)**. The number of passages varied with the concentration and the type of tomato paste; HB suspensions needing a much larger number of passages than CB tomato suspensions in order to reduce the particle size to similar values. The considerable difference in breakage behaviour between cold break and hot break paste confirms the earlier suggestion that the viscosity of the suspending medium plays a major role in determining the susceptibility to breakage of the particles in tomato suspensions. Cold break suspensions at different concentrations were subjected to a fixed number of passages through the homogeniser and the resulting particle size was found to be dependent on the concentration and the number of passages **(Paper III)**. In general, homogenisation decreased the particle size, while subsequent shearing of the suspensions resulted in an increase in particle size.
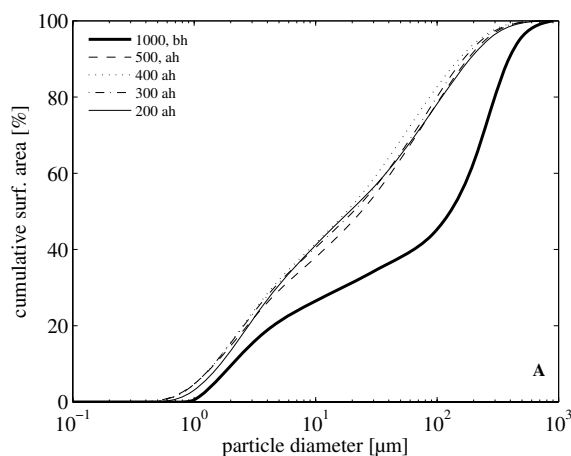
Figure 7. Particle size distribution of hot break tomato paste suspensions before homogenisation (bh, solid line) and after (ah) homogenisation, expressed as the cumulative surface area (%), as a function of the particle diameter (μm) for different concentrations, given in g/kg (see legend). (Adapted from **Paper II**).

A great deal of work has been devoted to extracting the maximum packing of particles (ϕ_m) from the PSD curves. The maximum packing of particles is of great importance in many fields of engineering, and it is directly related to rheological properties of a material (Farris, 1968). For example, optimising the PSD so that small particles occupy the spaces between large particles has the effect of decreasing the viscosity of the suspension by up

13

to a factor of 50, which can significantly reduced the pumping cost (Servais et al., 2002). It is also a key parameter in powder handling and processing as it determines the total volume occupied by the powder.

The maximum packing fraction is easily obtained in monodisperse suspensions, binary suspensions, i.e. particle populations with two discrete sizes, and ternary suspensions (three discrete particle sizes) (Lee, 1970). In continuous PSDs, the extraction of ϕ_m represents a complex mathematical problem, and the computational requirements make the solution difficult (Bierwagen & Saunders, 1974). Recently, ϕ_m was solved for a continuous PSD showing power law behaviour (Brouwers, 2006). For more complex PSDs, such as those found in food suspensions like tomato paste, no mathematical tools for the determination of the maximum packing of the particles are available today.

3.2.3   Concentration and volume fraction determination

The particle concentration is an important parameter determining the type of suspension, as well as the microstructure. There are different ways of expressing concentration, for example, based on the total solids, the water-insoluble solids or the volume fraction, but only the last one takes into account the microstructure of the suspension. The total solids and water-insoluble solids are, for example, not affected by processes that clearly change the microstructure of the suspensions, such as homogenisation. Volume fraction, on the other hand, is very sensitive to these changes. In this work, the volume fraction was determined by ultracentrifugation at 110,000 g. This value was used as Den Ouden (1995) and Rao (1999), claimed that very high centrifugation forces were needed to separate the solid and liquid phases in tomato paste. The drawback of using the centrifugation technique to determine the volume fraction is that the resulting value may be affected by deformation of the particles. Therefore, the volume fraction (ϕ) determined in the present work is indeed a compressive volume fraction and depends on morphological factors such as the PSD and the particle shape, as well as on the packing capacity and deformability. In this text, it will simply be referred to as volume fraction.

Suspensions can be classified as being dilute, in the transition region or as concentrated (Steeneken, 1989). Figure 8 shows illustrations of the arrangement of particles in the different regimes. In dilute systems, the particles are swollen to their equilibrium size, i.e.

14

they have maximum volume and are free to move in the suspension under Brownian forces. In the transition region, the particles are in contact with each other, but still have their maximum volume. In highly concentrated suspensions, the particles are deformed and fill the space available, and the suspension is thus fully packed. Another definition was given by Coussot and Ancey (1999), who described concentrated suspensions and granular pastes from a physical point of view, as "complex systems within which particles interact strongly, giving rise to viscosities much higher than the viscosity of the suspending media". In concentrated systems, the interactions and contact between particles clearly dominate over the Brownian forces.
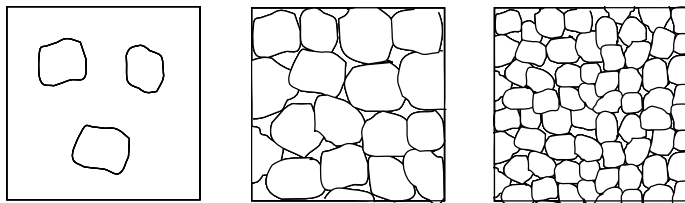
Figure 8. Concentration regime in suspensions. From left to right: dilute, transition and concentrated. (Adapted from Steeneken, 1989.)

In Figure 9, the volume occupied by the particles in tomato paste (100% bh), and in 50% tomato paste suspensions, before (bh) and after homogenisation (ah), is shown. It can be seen that homogenisation clearly increases the volume of particles in the suspension, at the same paste concentration.
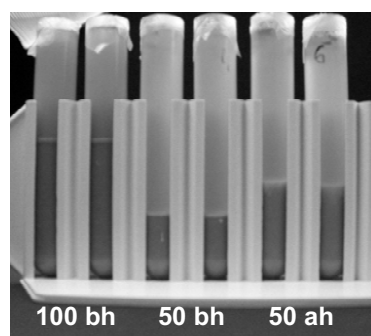
Figure 9. The volume fraction of tomato paste suspensions following ultracentrifugation at ~110,000 g for 20 min at 20ºC. The figure shows 100 and 50% paste before homogenisation (bh) and 50% paste after homogenisation (ah).

Different pastes show different behaviour with regard to the volume fraction as a function of the concentration of the paste. In Figure 10, the hot break (HB 22/24) and cold break (CB 36/38) suspensions described in **Paper II** are compared. The expected decrease in volume fraction due to dilution of the non-homogenised suspensions is shown as a dashed line, using the volume fraction from 100% paste as a reference. The behaviour of HB paste almost follows the predicted one, whereas CB suspensions seem to be more compressed by centrifugation. This shows that the volume fraction includes information about the ability of the particles to deform and pack at a given centrifugal force. The process of homogenisation clearly increases the volume fraction in both pastes. In **Paper I**, it was suggested that higher value of ϕ is related to a higher viscosity of the suspending medium. The case illustrated in Figure 10 is an extreme one, because the viscosity of the liquid phase in HB suspensions is several times greater than in CB suspensions (see Section 5.1.1). The higher viscosity of the liquid phase (η_s) may, to some extent, hinder the deformation of particles caused by centrifugal forces.
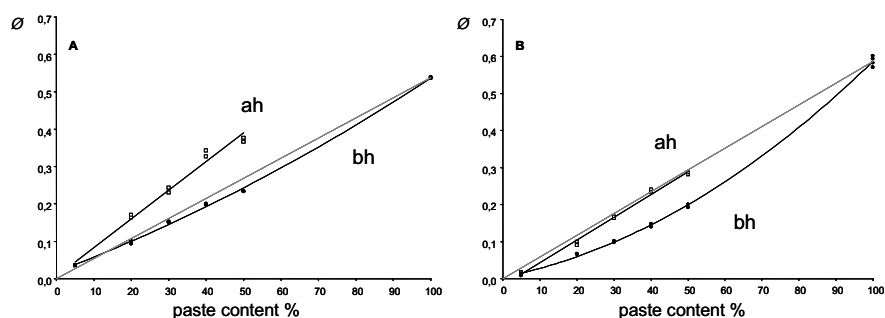
Figure 10. Comparison of the volume fraction obtained in (A) hot break 22/24 and (B) cold break 36/38 tomato paste suspensions at different concentrations, before and after homogenisation (**Paper II)**. The dashed line shows the predicted behaviour of non-homogenised suspensions.

3.3 Effect of concentration, particle size and shearing

Changes in microstructure due to processing, and vice versa, were studied in **Papers I-III**, by inducing or creating different types of arrangements in the suspensions studied, by means of varying the concentration and the particle size, and by shearing the structures formed. In the study described in **Paper I**, three HB tomato pastes were

studied as raw material in the production of a commercial ketchup. Slight variations in the composition, particle size distribution and particle susceptibility to breakage are reflected in the rheological properties of the final ketchups. In the study presented in **Paper II**, a more systematic approach was taken. Three different pastes were homogenised to sizes similar to those found in commercial ketchup, and the effects of both concentration and particle size on the time-dependent properties of the tomato suspensions were investigated. Finally, changes in the microstructure due to processing (homogenisation and shearing) were systematically studied on CB tomato paste suspensions at different concentrations (**Paper III).** Table 3 presents an overview of the studies described in each of the papers. **Paper IV** is included for completeness.

Table 3. Overview of the experimental studies described in **Papers I-IV**, including the type of paste used, range of concentrations studied and the degree of homogenisation applied. The type of rheological measurements performed in each study is also given.

Factor	Paper I	Paper II	Paper III	Paper IV
Paste type	3 HB	2 HB and 1 CB	1 CB	1 HB and 1 CB
Concentration g/kg	1000, 400, 300	1000, 500, 400, 300, 200	400, 300, 100	1000, 500, 400, 300
Homogenisation	300 g/kg to ketchup size	500-200 g/kg to ketchup size	400-100 g/kg 3 degrees	-
Shearing	-	During measurements	1 h, magnetic stirrer	-
Measurements				
Flow curve	+	+	-	+
Creep	-	+	-	-
Dynamic	+	-	+	+
Yield stress	+	+	-	+

Effect of concentration on the particle size

In this study, the concentration of tomato suspensions was expressed in terms of the volume fraction, ϕ, instead of the more common forms, Brix degree, water-insoluble solids or total solids, because these are not related to the microstructure. The effect of concentration on the microstructure of tomato suspensions can not be studied using microscopy, because dilution of the samples is required, and their arrangement in the suspension would thus be disrupted. Therefore, the effects of concentration were investigated in terms of other parameters, such as the rheological properties (Sections 4.2

and 5.1). Moreover, the influence of the concentration on the performance of the homogeniser, in decreasing the particle size to a set value, was studied. The last point will be discussed in this section.

In **Paper II**, the number of passages through the homogeniser required to decrease the particle size of different tomato pastes to a set value, was determined, taking into account the concentration of the suspensions and the type of paste (Fig. 11A). In general, fewer passages were required with decreasing concentration. The effect of a fixed number of passages on the particle size of the suspension is shown in Figure 11B, for different concentrations. The decrease in particle size in the more concentrated sample (400 g/kg) is less pronounced than in the others at a given number of passages. The changes following homogenisation differ considerably between HB and CB suspensions, the latter requiring much fewer passages to break down the particles. This may also be related to the lower viscosity of the suspending medium (η_s), in CB suspensions.
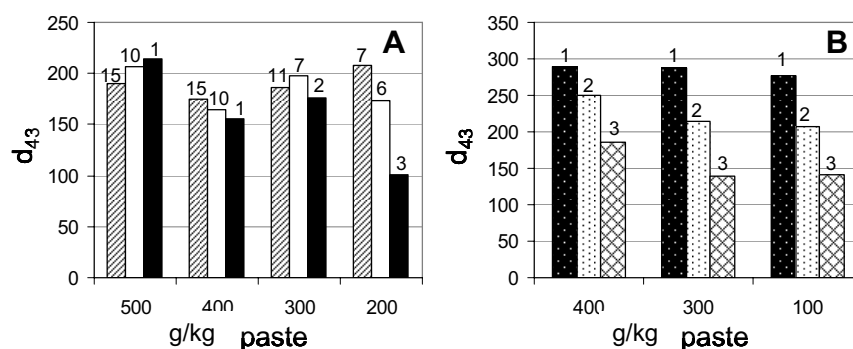
Figure 11. Volume-based diameter (d_{43}, µm) as a function of the concentration of the paste (g/kg), for different numbers of passages through the homogeniser (given above each column). A) Adapted from **Paper II**: HB 28/30 ▨, HB 22/24 ☐, and CB 36/38 ■. B) Adapted from **Paper III**, CB 36/38.

Finally, it is interesting to note that the behaviour of suspensions during the process of homogenisation is markedly different from that of emulsions. In emulsions the relevant parameter in decreasing the size of the particles is the homogenisation pressure (Tornberg, 1978), while the size of the particles remains approximately constant after repeated passage at the same pressure. This is not the case in suspensions and Figure 11B clearly shows the importance of the number of passages in determining the final size of the particles.

18

Figure 12. Effect of homogenisation and subsequent shearing on the microstructure of 10% cold break tomato paste suspensions before homogenisation (H0) and after 1, 2 and 3 passages (H1-H3) through the homogeniser (pressure ~90 bar). (Adapted from **Paper III**.) The scale bar is 250 μm.

Effect of homogenisation and subsequent shearing

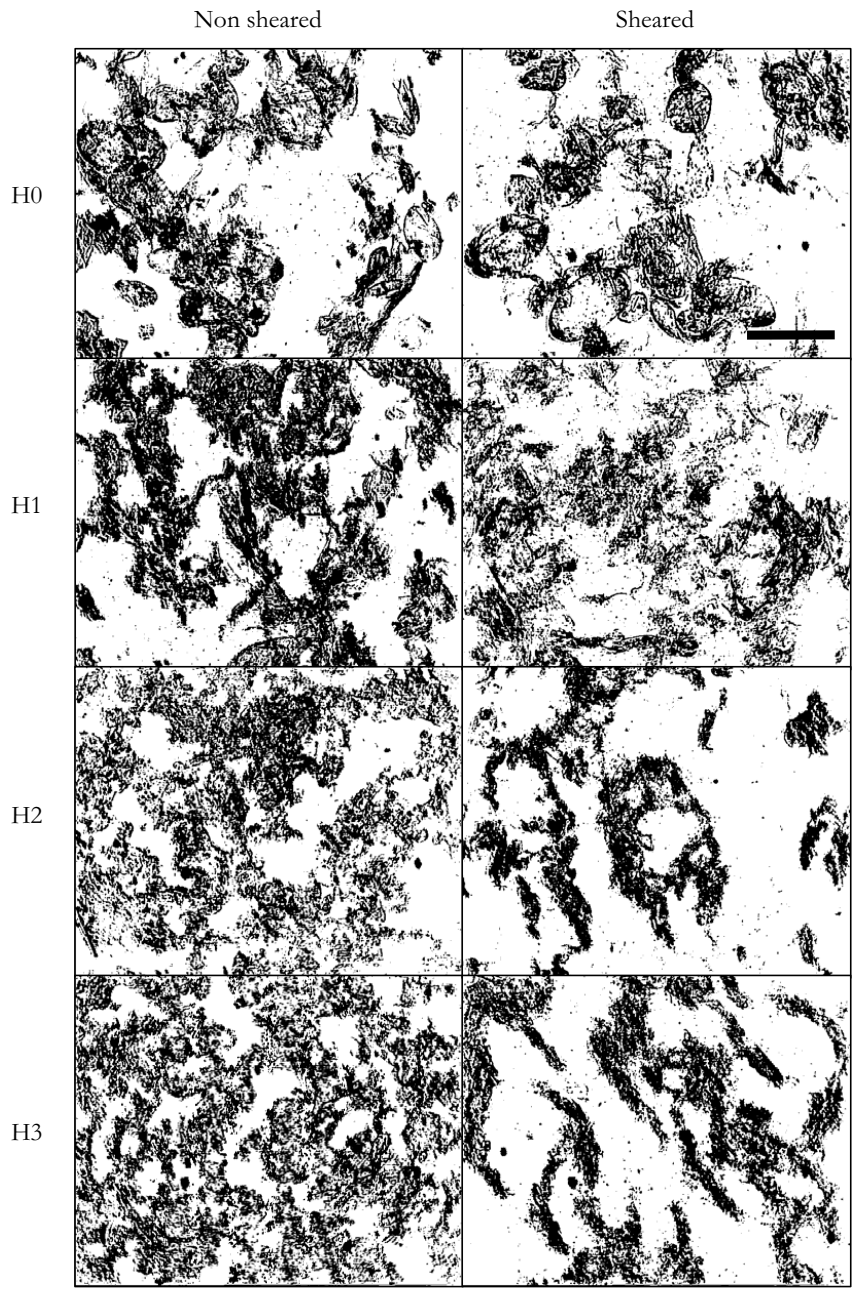Homogenisation and subsequent shearing of the suspensions cause substantial changes in the microstructure of the suspensions, as can be seen in Figure 12, for 10% CB suspensions (**Paper III**). The series of images on the left show the successive creation of an evenly distributed network by passing the suspension through the homogeniser several times. A decrease in the particle size is evident, which is accompanied by an increase in the surface area covered by the particles. Subsequent shearing of the suspensions (right-hand images in Fig. 12) had no visible influence on the surface area at a low degree of homogenisation, but for the well homogenised suspensions the structure of the suspensions was considerably different after shearing. In fact, in the most homogenised and sheared suspensions the individual particles tended to aggregate forming heterogeneous regions with densely packed flocs, resulting in a completely different type of network. These observations suggest that the process of homogenisation creates a smooth network of finer particles that is easily disrupted by prolonged shearing.
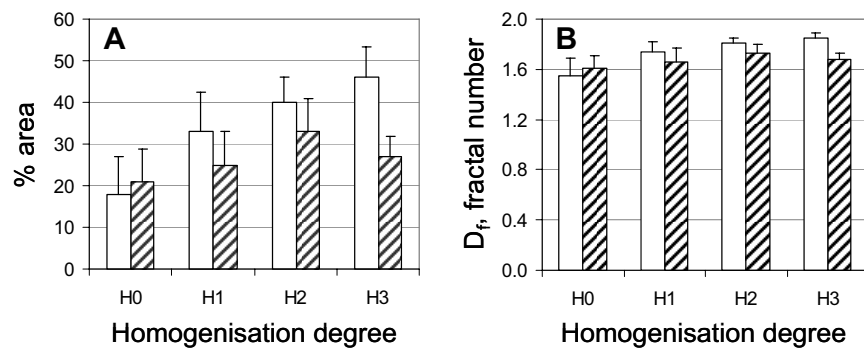
Figure 13. A) Percentage area covered by the particles and B) fractal number associated with the 2-dimensional images, as a function of the degree of homogenisation in 10% tomato paste suspensions. Results are shown for non-sheared (□) and sheared samples (▨).(Adapted from **Paper III**, CB 36/38.)

The different features revealed in these microscopic images can be quantified using image analysis, and the area covered by the particles, the fractal number and the size of the pores or the distance between particles and flocs were determined (the image analysis procedure is described in Section 3.2.1). The area covered by the particles and the fractal number (Fig. 13) exhibit similar behaviour upon homogenisation and subsequent

shearing. Both variables are found to increase with the degree of homogenisation, whereas shearing has a negative effect on their values. The structure of the unsheared well-homogenised suspensions shows a high degree of fractality, and probably consists of dense areas connected by thin linkages (H3). On shearing, the network is probably disrupted first at these linkages, followed by the densification of the floc structure and the growth of the floc size (H3-SH).

The fractality of the network structure is one of the few existing ways to relate microstructure and rheology, and a number of scaling laws relating them have been developed for colloidal suspensions and gels (Buscall et al., 1987, Buscall et al., 1988) and more recently for fat crystals (Narine & Marangoni, 1999). The applicability of such laws relating microstructure and rheology in tomato suspensions will be discussed in Chapter 4.

The average separation between particles or aggregates, as well as the porosity of the network, is of importance in understanding the rheological behaviour and the microstructure of the suspensions. The distance between the particles and/or the distribution of pores in the network is observed to change on homogenisation followed by shearing (Fig. 12, Fig. 14). In the non-homogenised samples, the average distance between the particles (i.e. whole cells) is about 135 μm. During homogenisation, the microstructure of the network changes, and this change is accompanied by the formation of smaller pores. At a low degree of homogenisation (H1) only 40% of the pores are below 45 μm, having an average size of about 80 μm. In the highly homogenised system (H3), the averaged pore size has decreased to 54 μm and more than 50% of the pores are now below 45 μm. Successive shearing of this network leads to the formation of aggregates/flocs, separated by a distance of the order of 100 μm. Note, however, that in the sheared samples, the distance between particles, i.e. whole cells or aggregates, seems to be independent of the degree of homogenisation, although the shape, size and distribution of the particles are drastically different.
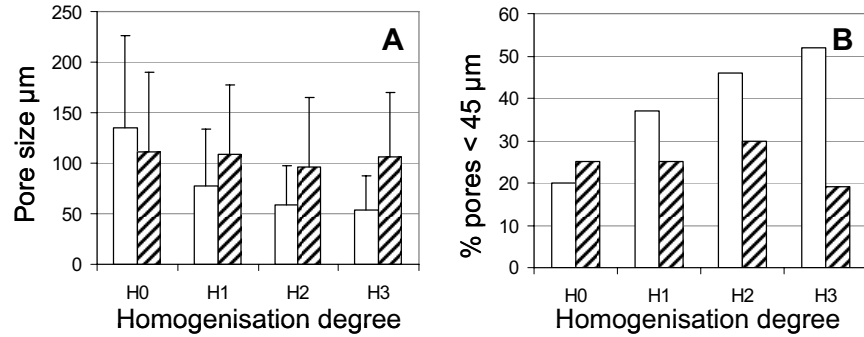
Figure 14. A) Pore size (or distance between particles and/or flocs), and B) percentage of pores with a size below 45 μm, as a function of the degree of homogenisation in 10% tomato paste suspensions. Results are shown for non-sheared (▫) and sheared samples (▨).(Adapted from **Paper III**, CB 36/38.)

Following prolonged shearing, the network of tomato homogenates rearranges, forming discrete, closely packed flocs, consisting of aggregates of small individual particles. These flocs are easily oriented in the direction of the flow (in Fig. 12, at about 45°) and have an aspect ratio of the order of ~10, whereas that of the individual particles is about ~1.5. Mills et al. (1991) studied the effect of prolonged shearing in model colloid suspensions and found that the particles tended to form flocs or aggregates, which led to a significant decrease in yield stress, apparent viscosity and shear modulus. They reported that the size of the aggregates was independent of the initial volume fraction, and probably determined by the size of the individual particles.

22

4. Mechanical Spectra of Concentrated Suspensions

The word "rheology" was coined by Bingham in the 1920s and comes from the Greek, where *rheos-* means "current or flow" and *logos-* means "word or science". Rheology is thus the study of the deformation and flow of matter in response to a mechanical force. In this chapter , measurements based on deformation caused by oscillatory shear are discussed. In the next chapter (Chapter 5) flow behaviour upon the application of steady shear is discussed.

An overview of the rheological measurements performed and the type of measurement system used in each of the studies is given in Table 4.

Table 4. Overview of the rheological measurements reported in **Papers I-IV**. The type of geometries used in each study is also given.

	Paper I	*Paper II*	*Paper III*	*Paper IV*
Geometries used				
Concentric cylinder	-	-	-	+
Vane	+	+	+	+
Outer vane	-	-	-	+
Tube viscometer	-	-	-	+
Measurements				
Flow curve	+	+	-	+
Creep	-	+	-	-
Dynamic	+	-	+	+
Yield stress	+	+	-	+

4.1 Dynamic oscillatory rheology

A common way of investigating the microstructure of complex fluids is the application of small-amplitude oscillatory shearing, which does not significantly deform the microstructure of the fluid being tested. Most food materials are considered to be

complex fluids, meaning that they have mechanical properties between those of ordinary liquids and ordinary solids (Larsson, 1999).

4.1.1 Strain/stress sweep tests

In oscillatory testing, a sample is deformed sinusoidally by the application of small-amplitude, oscillatory deformations in a simple shear field. When the material is tested in the linear viscoelastic regime, its mechanical properties do not depend on the magnitude of the strain or stress applied. The linear viscoelastic region can be determined experimentally for each material, by means of a stress/strain sweep test. This test consists of increasing the magnitude of the stress or strain, while keeping the frequency of oscillation constant, usually 1 Hz (Fig. 15). When the material enters the non-linear region, the material properties become dependent on the level of stress/strain applied. In food materials, strains are often kept below 1% to avoid non-linear effects (Steffe, 1996).
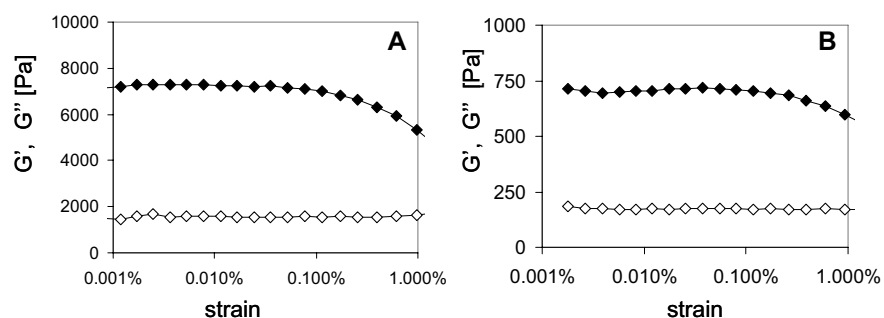
Figure 15. Results of typical strain-sweep measurements performed at a frequency of 1 Hz, for A) tomato paste and B) ketchup. The elastic modulus G' (♦) and the loss modulus G" (◊) are expressed in Pa. **(From Paper I)**.

The non-linear viscoelasticity of foods i.e. the behaviour at large deformation, may be relevant in many processes, such as swallowing during the sensory evaluation of food, but in such measurements the microstructure of the material is disrupted. Therefore, only the linear oscillatory rheology of tomato suspensions at small deformations, which yields structural information of the "intact" network structure, was studied in this work.

In the linear region, the sinusoidally varying stress (σ) can be written:

$$\sigma(t) = \gamma_0 [G'(\omega)\sin(\omega t) + G''(\omega)\sin(\omega t)] \tag{3}$$

where ω is the frequency of oscillation, and G' is the storage or elastic modulus, and G'' is the loss modulus. For solid-like materials $G' >> G''$, whereas for liquid-like materials $G' << G''$. The complex modulus, G^*, is defined by $G^* = G' + iG''$, and the complex viscosity is thus defined by $\eta^* = |G^*(\omega)|/\omega$.

4.1.2   Mechanical spectra in the linear viscoelastic region

The mechanical spectrum of dilute model solutions is predicted by the general linear model to scale with the frequency, as $G' \propto \omega^{2.0}$ and $G'' \propto \omega^{1.0}$, with the loss modulus being much higher than the elastic modulus: $G'' > G'$. The power law is obeyed in the low-frequency region, $\omega \rightarrow 0$. The mechanical spectrum of a gel is instead expected to be independent of the frequency ω (Ferry, 1980; Ross-Murphy, 1988, Fig. 16). Recently, it has been shown experimentally that during the sol-gel transition $G' \propto \omega^{0.5}$ (Liu et al., 2003).
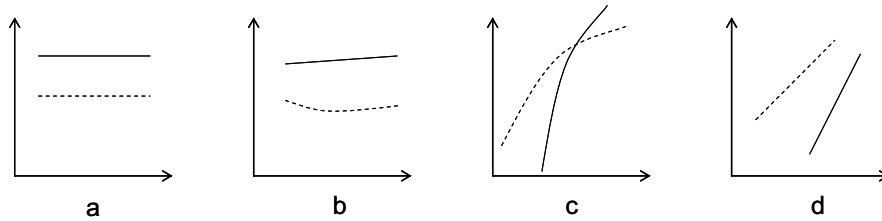
Figure 16. Typical mechanical spectra showing elastic modulus and the loss modulus as a function of frequency, for: A) a solid, B) a weak gel, C) a concentrated suspension and D) a liquid. The elastic modulus G' is represented by a solid line and the loss modulus G'' is represented by a dashed line. (Adapted from Ross-Murphy, 1988.)

Real fluids, such as semi-liquid or semi-solid foods, exhibit intermediate mechanical spectra to those of model solids and liquids. **Paper I** describes the frequency-dependent behaviour of tomato pastes and their corresponding ketchups (Fig. 17). Tomato pastes, for example, are found to behave as weak gels, $G' > G''$ over all the frequencies studied

25

(0.01-10 Hz). At low frequencies, ω <0.1, the loss modulus is almost independent of the frequency, whereas G' increases slightly with ω. At frequencies above this value (ω > 0.1), G' and G'' scale with the frequency as $\omega^{0.1}$ and $\omega^{0.2}$, respectively. The corresponding ketchups also show solid-like behaviour, with $G' > G''$, and in the low-frequency region, G'' shows a minimum, which is also typical of weak gels and highly concentrated suspensions. At higher frequencies (ω >0.1), G' and G'' scale as $\omega^{0.1}$ and $\omega^{0.3}$, respectively.
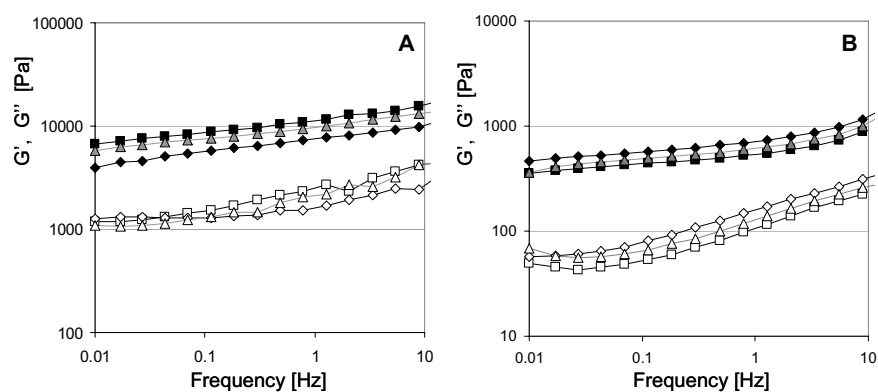
Figure 17. Typical mechanical spectra for A) three tomato pastes and B) the corresponding ketchups. The elastic modulus (filled symbols) and the loss modulus (open symbols) are shown as a function of the frequency. Note that the scales in A and B are different. (Adapted from **Paper I)**.

The shape of the $G'(\omega)$ and $G''(\omega)$ curves shown in Fig. 17 does not seem to vary between the different types of paste, but varies slightly between pastes and ketchup. This suggests that processing, i.e. dilution and homogenisation, does not affect the frequency dependence of tomato suspensions to any great extent. In the study reported in **Paper III** it was found that the mechanical spectra of unsheared and sheared tomato suspensions, at different concentrations, and at several degrees of homogenisation followed similar trends. However, the magnitude of the elastic and loss moduli varied with the type of paste, concentration, degree of homogenisation and prolonged shearing.

As an example of non-gelling suspensions, the mechanical spectra of two potato fibre suspensions, at low and high concentration, are shown in Fig. 18. The low-concentration sample shows the typical behaviour of a diluted suspension, and behaves as a liquid

($G'' > G'$) at all frequencies ($\omega = 0.01\text{-}10$ Hz). It shows stronger frequency dependence than the tomato suspensions, with $G' \propto \omega^{0.7}$ and $G'' \propto \omega^{0.7}$. Increasing the concentration of potato fibres to 6.5% leads to more gel-like behaviour at low frequencies, whereas at about 1 Hz the viscous behaviour of the suspension takes over. The frequency dependence is now $G' \propto \omega^{0.4}$ and $G'' \propto \omega^{0.6}$, still much stronger than in tomato products. These two potato suspensions were used in the pumping experiment reported in **Paper IV**.
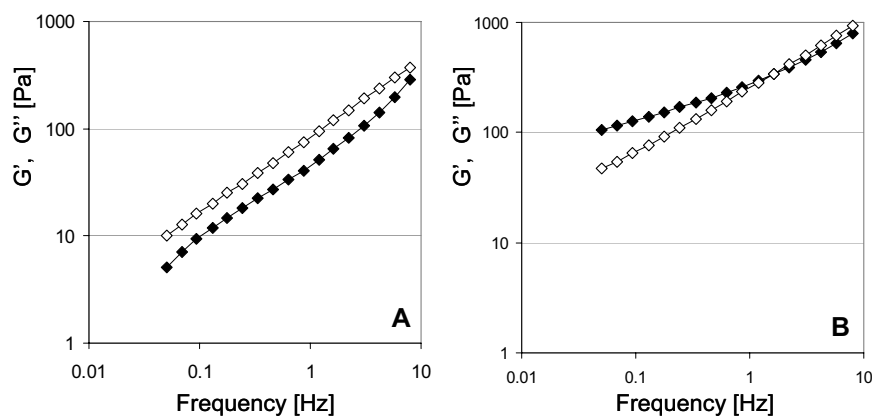
Figure 18. Mechanical spectra for dried potato fibre suspended in 860 mPa s syrup, A) at low concentration (4.5%), and B) at high concentration (6.5 %). The elastic modulus (filled symbols) and the loss modulus (open symbols) are given as a function of the frequency . Note that the scales in A and B are different. (Data for two of the suspensions reported in **Paper IV**.)

4.2 Effect of concentration, particle size and shearing

The viscoelastic behaviour of suspensions is determined by the particle size distribution and shape, as well as the volume fraction of particles (Nakajima & Harrell, 2001, Servais et al., 2002) and the particle-particle interactions (Shah et al., 2003) as well as the spatial arrangement of the particles; in other words, the viscoelastic properties are dependent on the microstructure of the suspension.

Some recent experiments show that small changes in the microstructure can have a drastic effect on the mechanical properties of colloidal suspensions and gels. For

27

example, Channell et al. (2000) induced heterogeneities in the microstructure of flocculated alumina suspensions and arrived at the conclusion that the yield stress determined by uniaxial compression was more sensitive to heterogeneities than the elastic shear modulus. Miller et al. (1996) also found that the suspensions became more compressible as the particle size is increased.

The fractal description of the microstructure and its relation to rheological properties are well established for relatively dilute colloid systems (Muthkumar, 1985). In fat crystals, the fractal description holds for fat concentrations up to a volume fraction of ~0.7 (Narine & Marangoni, 1999), and can be expressed as:

$$G' = \alpha \phi^{\beta} , \tag{4}$$

where α is a constant that depends on the size of the particles and on the interactions between them, ϕ is the volume fraction of particles, and $\beta = 1/(d - D_f)$ is an exponent that depends on d, the Euclidean dimension of the network (usually $d = 3$), and D_f, the fractal dimension of the network.

The fractal scaling behaviour should be interpreted with care in highly concentrated gels (Wyss et al., 2005). Buscall et al. (1987, 1988) found exponents much higher than 3 for the dependence of the elastic modulus on the concentration, and proposed that the networks had a highly non-uniform, heterogeneous structure comprising a collection of interconnected fractal aggregates.

The influence of the microstructure on the rheology of the suspensions is less well understood for highly concentrated suspensions, probably due to the fact that the number of techniques available to investigate the microstructure of such suspensions is rather limited (Wyss et al., 2005), and also because there is no standardised way of quantifying the microstructure and relating it to the macroscopic properties of the material, such as the rheological behaviour.

The microstructural changes that tomato suspensions undergo upon homogenisation and subsequent shearing have been analysed in relation to their mechanical properties, taking into account the particle size and the concentration of the suspensions, and are described

in **Paper III**. The ratio of the percentage of fine to coarse particles (f/c) is used as a parameter to represent the PSD of the suspensions investigated. The PSD was found to vary with the degree of homogenisation and, to a lesser extent, with subsequent shearing.

The particle size of the coarse fraction (> 10 μm) and the compressed volume fraction were the most relevant parameters in defining the elastic modulus, G′, and an empirical equation (Eq. 5) was found to accurately describe the whole set of data (R^2>99.3%, p<0.001), as is shown in Fig. 19,

$$\log G' = 3.75 + \log \phi^{2.47} + 4120 d_{32,coarse} . \qquad (5)$$
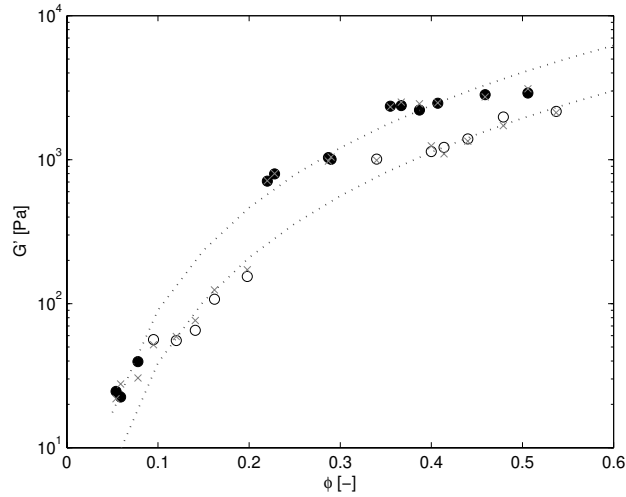
Figure 19. Linear elastic modulus (G′, ω=1Hz) as a function of the volume fraction (ϕ) in suspensions with predominantly coarse (f/c<1, ●) or fine (1<f/c<3, ○) particles. The values fitted using Equation 5 are also shown (x). The dotted lines represent the fits to $G' = \alpha \phi^{\beta}$. (Adapted from **Paper III**.)

The elastic modulus was also modelled following the fractal scaling (Eq. 4). The data plotted in Figure 19 indicate that suspensions with predominantly coarse particles (100 μm, f/c<1) exhibit higher values of G' than suspensions with predominantly fine particles (30 μm, f/c>1), at a given volume fraction.

The values of α in Equation 4 have values of ~20000 and ~10000, for coarse and fine fractions, respectively. The fractal number was not substantially different in the coarse and fine fractions, having a value of D_f ~2.58, which is comparable to the averaged value obtained from the image analysis of the 10% tomato paste suspensions (Fig. 13B). Note that the images are in 2-D. The averaged D_f value for fine and coarse 10% suspensions can be calculated and converted to 3-D, by assuming that the suspensions are isotropic. This gives a value of 2.41 for the coarse suspensions (f/c<1) and 2.64 for the fine suspensions (1<f/c<3), which are in qualitative agreement with the fitted value. However, it is not possible to confirm the fractal behaviour of the highly concentrated suspensions, and extrapolating the results from the semi-diluted regime to higher concentrations is not sufficiently accurate. Moreover, the determination of the volume fraction involves some compression of the network, and ϕ is then the volume of the deformed particles and not necessarily the cumulative volume of the primary fractal elements. Even with the above mentioned limitations, the power-law scaling holds for a large range of ϕ, PSD and particle shapes in tomato suspensions.
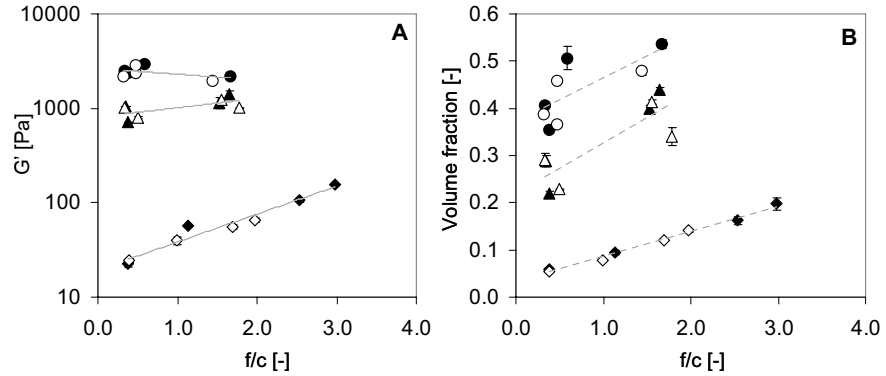
Figure 20. A) Elastic modulus and B) volume fraction determined by centrifugation, as a function of the ratio of fine-to-coarse particles (f/c) for 10, 30 and 40% tomato paste suspensions (♦, ▲, ●, respectively). Filled symbols represent samples before shearing and empty symbols samples that were subjected to prolonged shearing. The lines are a guide to the eye. (Adapted from **Paper III**.)

The concentration has a strong impact on both the rheological behaviour of the suspensions and the effectiveness of processing. In semi-diluted regimes, such as 10%, the particles are probably swollen to equilibrium (Steeneken, 1989) and form a more

heterogeneous network consisting of a collection of particles or aggregates/flocs, with large pores in between (Fig. 13A). The rheological properties (G′) of this type of suspension depend linearly on f/c, whereas this does not seem to be the case for more concentrated suspensions, being more independent of f/c (Fig. 20A). The results of the present work suggest that the 30 and 40% tomato paste suspensions instead form a continuous particulate network, where the particles fill the available space and are probably not swollen to equilibrium, but exist as more deformed particles

The volume fraction was found to be more sensitive to changes in the microstructure of highly concentrated suspensions than the elastic modulus (Fig. 20B). The reason for this could be that the deformability of the particles comes more into play in more concentrated suspensions, as pointed out by Steeneken (1989). The deformability of the particles is a key parameter in explaining why the presence of heterogeneities in the microstructure could be measured using compressive yield stress (by centrifugation), while the shear modulus could not differentiate between different types of microstructures according to Channell et al. (2000). In the present study, large particles, aggregates or flocs, and large pores or voids in the network caused heterogeneities in the microstructure of the suspensions. Since the volume fraction was determined by ultracentrifugation, i.e. uniaxial compression at a given speed (~110,000 g), it could be affected by the compressive strength of the different networks, i.e. by the heterogeneities induced by homogenisation and subsequent shearing. However, those changes introduced by processing may not alter the number of junction points in the network, especially in the more concentrated suspensions where particles are physically touching each other and filling the spaces, thus giving similar G′ values in the dynamic shear measurements.

5. Flow Behaviour of Concentrated Suspensions

The flow behaviour of the materials can be described by rheological models. Rheological models describe the relationship between the shear stress (σ) and the shear rate ($\dot{\gamma}$). Newtonian fluids show a linear relationship between these variables, while non-Newtonian fluids exhibit a non-linear dependence.

$$\sigma = \eta(\dot{\gamma})\dot{\gamma} \tag{6}$$

Tomato products exhibit pronounced non-Newtonian effects, e.g. yield stress, shear-thinning behaviour and shear history dependence (Rao, 1999). The rheological properties of tomato products have been described using the popular power-law equation or, when the yield stress is taken into account, the Bingham, Herschel-Bulkley and/or Casson models (Table 5). The applicability of each of these models depends on the range of shear rates considered.

Table 5. Some typical rheological models used to describe the viscosity of tomato products

Power law	$\sigma = K\dot{\gamma}^n$	Bingham	$\sigma = \sigma_y + \mu\dot{\gamma}$
Herschel Bulkley	$\sigma = \sigma_y + K\dot{\gamma}^n$	Casson	$\sigma^{0.5} = \sigma_y^{0.5} + K^{0.5}\dot{\gamma}^{0.5}$

5.1 Suspension rheology

The rheological behaviour of dilute suspensions and colloid dispersions, and some model concentrated suspensions, is relatively well understood (Coussot & Ancey, 1999). Already in the early 1900s, Einstein proposed that the viscosity of a dilute suspension of hard spheres ($\phi \leq 0.03$), assuming no interactions, was governed by

$$\eta = \eta_s(1 + 2.5\phi) \tag{7}$$

Hydrodynamic effects appear when two spheres are close enough that the flow around one of them is influenced by the presence of the other. The Krieger-Dougherty equation appears to described the viscosity of more concentrated suspensions of hard spheres (ϕ <0.63), at low shear rates $\dot{\gamma} \rightarrow 0$, when hydrodynamic effects dominate and particle interactions are negligible.

$$\eta = \eta_s \left(1 - \frac{\phi}{\phi_m} \right)^{-2.5\phi_m} \tag{8}$$

In highly concentrated suspensions, the interaction between particles dominates over the hydrodynamic forces, especially at low shear rates, and the material exhibits a yield stress. If the particles are large, and contact with other particles occurs, frictional and collision effects may come into play. Coussot and Ancey (1999) proposed a classification of the different rheological regimes from a physical point of view, considering both the concentration and the shear rate (Fig. 21). They defined a concentrated suspension as that in which particle interactions play a major role in the rheological behaviour of the suspension, giving rise to a viscosity that is several orders of magnitude higher than the viscosity of the interstitial suspending medium (η_s).
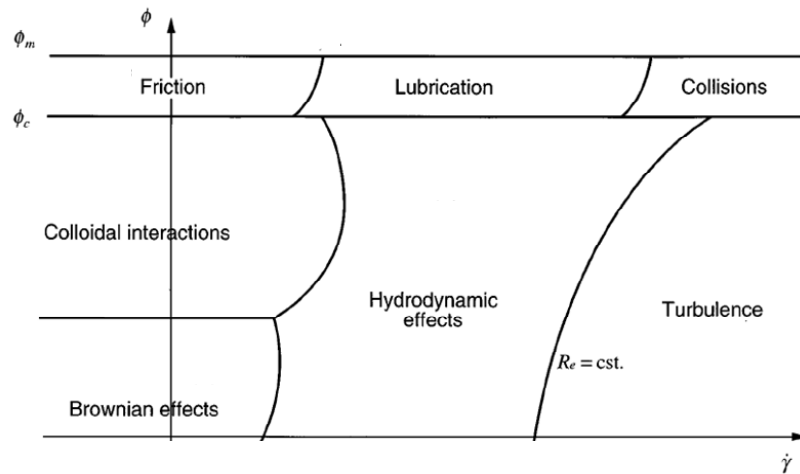

Figure 21. Classification of forces involve in different rheological regimes as a function of the shear rate and the volume fraction. (Adapted from Coussot & Ancey, 1999.)

34

It is also important to note that several practical difficulties are encountered in rheological measurements of highly concentrated suspensions and gels, for example poor reproducibility, sensitivity to shear history and to the preparation of samples, and slip (Larsson, 1999; Kalyon, 2005). Up to 50% variability has been reported in the rheological properties of wheat starch at high concentrations (Steeneken, 1989), and between 15 and 30% in the determination of yield stress in model colloidal suspensions (Buscall et al., 1987). Measurements performed under similar experimental conditions, but in different geometries, do not always agree (Plucinski et al., 1998), and hence the comparison and/or prediction of rheological properties from one instrument to another is difficult. In section 5.2, some considerations regarding measurement systems will be discussed.

5.1.1   Rheological behaviour of tomato products

Den Ouden (1995) reported viscosities of the supernatant of the order of ~20 mPa s for HB tomato paste and ~4 mPa s for CB tomato paste, and claimed that the contribution of the suspending medium to the apparent viscosity of tomato paste was very little, and that the tomato particles and the fibre network accounted for the extremely high apparent viscosities, especially at low shear rates. In the present work, the viscosity of the suspending medium was below 7 mPa s for the CB suspensions and below 20 mPa s for the diluted HB suspensions (Fig. 22).

The behaviour of the viscosity of the supernatant upon dilution is, however, markedly different in hot and cold break suspensions, and while η_s resembles that of a sucrose solution in CB samples, it increases much more steeply in HB samples. Note that the viscosity of the supernatant in 100% HB paste is not included in Figure 22 because it exhibits non-Newtonian behaviour, but for comparison, at $\dot{\gamma} = 10$ s^{-1}, η_s ~300 mPa s, for Brix degrees between 20 and 30. The main difference between hot and cold break processing is that the former is carried out at high temperatures (> 85°C), while the latter is only subjected to low temperatures (< 70°C). Low temperatures allow a certain degree of pectin degradation because of the slow and incomplete inactivation of the enzymes involved, i.e. pectin methyl esterase and polygalacturonase. Fito et al. (1983) reported that the content of soluble pectins present in CB pastes was significantly lower than in HB pastes, and several authors have suggested that the presence of soluble pectins is a key

parameter in determining the viscosity of tomato paste (Thakur et al., 1996; Chou & Kokini, 1987; Hurtado et al., 2002).
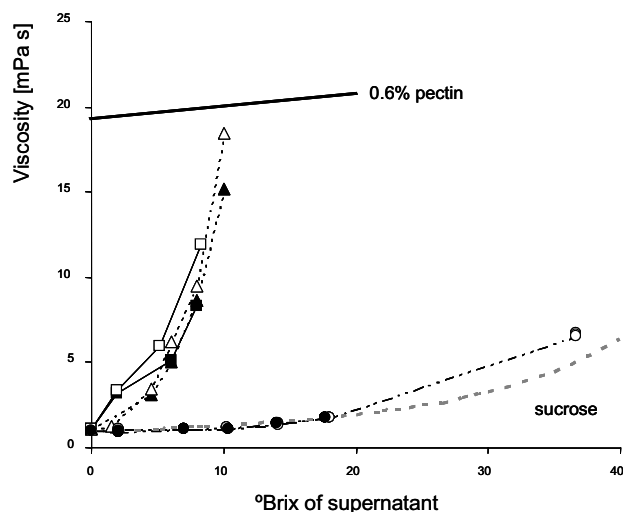

Figure 22. Supernatant viscosity as a function of the Brix degree of the solution, determined at a shear range of 10 s^{-1}, in the supernatant of three tomato pastes: HB 28-30 (■), HB 22-24 (▲) and CB 36-38 (●), at different concentrations. Filled and empty symbols show data for suspensions before and after homogenisation, respectively. For comparison, the viscosity of a sucrose solution and a sucrose solution with 0.6% pectin added is also shown.

However, the extremely high viscosity that tomato paste exhibits at low shear rates ($\eta \sim 10^6$ Pa s, Fig. 23) makes the direct contribution of pectins almost negligible, as pointed out by Den Ouden (1995). This work suggests that the soluble pectin content or, in other words, the viscosity of the liquid phase in tomato paste, contributes indirectly to the viscosity by affecting the microstructure of the suspensions. Observations such as CB pastes being more compressible, and their constituent particles more easily broken down by homogenisation, in contrast to HB paste, have been repeatedly made in this work (see Sections 3.2.3 and 3.3).

The typical flow behaviour of tomato suspensions is shown in Figure 23, as the apparent shear viscosity as a function of the shear rate. An initial Newtonian plateau is followed by a shear-thinning region, which seems to change slope at shear rates around 0.1 to 1 s^{-1}. In **Paper I**, the Carreau model (Eq. 9) was found to describe the flow behaviour of tomato

36

pastes rather accurately, and the values of the parameters were of similar magnitudes to those reported by others (Valencia et al., 2003); i.e. the zero-shear viscosity $\eta_0 \sim 10^6$ Pa s, the time constant $\lambda \sim 10^4$ s, and the exponent N~0.4.

$$\eta = \frac{\eta_0}{\left[1 + \left(\lambda\dot{\gamma}\right)^2\right]^N} \tag{9}$$

Whether or not the flow behaviour of tomato food systems is better represented by the zero-shear viscosity or by the presence of a yield stress will be further discussed in the following section.
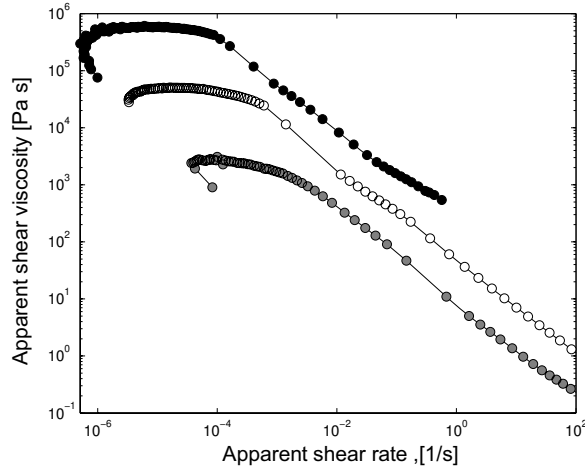
Figure 23. Typical apparent shear viscosity as a function of the shear rate in tomato paste (●), ketchup before homogenisation (◎) and ketchup after homogenisation (○). (Adapted from **Paper I**.)

5.1.2 Yield stress

Yield stress is the minimum stress required to achieve flow. When the stress applied to a material is below a certain value ($\sigma < \sigma_y$), the material experiences little or no deformation, and behaves as a Hookean solid. When the stress exceeds a certain value ($\sigma > \sigma_y$), the material begins to flow. The yield stress arises from the balance between external and internal forces (Whittle & Dickinson, 1998; Coussot & Ancey, 1999), i.e. the yield stress exists while the external forces and internal fluctuations, i.e. Brownian forces, are insufficient to significantly disrupt the network, $E_{external} + kT << E_{network}$. In fluids at rest,

such as polymers and dilute suspensions (particle size < 10 μm), the Brownian force dominates (kT), but this effect diminishes with increasing particle number and size, as is the case in concentrated suspensions.

The presence of a yield stress is a characteristic of concentrated suspensions, and it is related to the strength of the network structure, which in turn results from attractive particle-particle interactions (Larsson, 1999; Coussot & Ancey, 1999). The magnitude of the yield stress is affected by a number of factors, such as the density of the network, particle concentration, particle size and shape, among others (Dzuy & Boger, 1983).

There has been a long, controversial debate in the literature driven by the articles published by Barnes and Walters (1985) and Barnes (1999) questioning the concept of yield stress. The authors claimed that the yield stress does not really exist, but it is a consequence of the limitations of the measurement system, and when it is possible to make measurements at very low shear rates, a large but finite viscosity is always found, i.e. zero-shear viscosity (η_0).

The findings of the present work, however, support the idea expressed by Buscall et al. (1987) among others, that yield stress virtually exists in concentrated systems since they behave so shear-thinning that a small increase in shear stress, in a critical range, leads to a decrease in viscosity from a very large value ($\sim 10^6$) to a value of the order of 1 Pa s.

In **Paper II**, data are presented for tomato suspensions subjected to low shear rates. The first part of the study was dedicated to the identification of the yield stress using creep measurements. Figure 24A shows the typical response of the transient shear rate as a function of shearing time. The response is different when different levels of stress are applied, and three kinds of behaviour have been identified: a) below the yield stress ($\sigma < \sigma_y$), b) at low stresses ($\sigma \sim \sigma_y$) and c) at high stresses ($\sigma >> \sigma_y$):

   a) for $\sigma < \sigma_y$, the initial response of the system is to exhibit a shear rate below 10^{-2} s^{-1} followed, at later times, by a marked decrease in the shear rate over several decades down to $\sim 10^{-4}$ s^{-1}, where the measurements become unstable, and the system basically deforms as a solid.

b) for $\sigma \sim \sigma_y$, the system will begin to flow, at an initial shear rates ranging from 10^{-2} s^{-1} to 10^{-1} s^{-1}. The variation in the shear rate with time is then limited to values within the same order of magnitude.

c) for $\sigma \gg \sigma_y$, the system begins to flow at shear rates ranging from 10^{-1} s^{-1} to 10^0 s^{-1}, and at long times, a sudden increase in the shear rate over one or more decades, up to 10^1 s^{-1}, takes place.
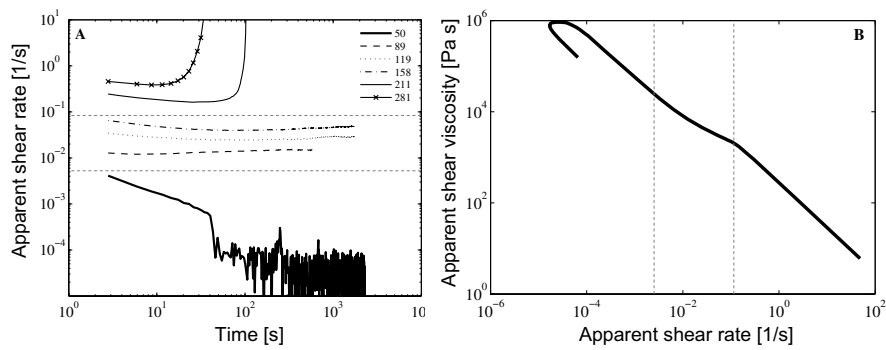
Figure 24. A) Evolution of the shear rate (s^{-1}) as a function of the shearing time at constant stress (see legend), and B) apparent shear viscosity as a function of the shear rate, of a HB tomato paste. The dashed grey lines represent the intervals of shear rates limiting the different rheological responses, see the text. (Adapted from **Paper II**.)

The different behaviour described above was observed in HB and CB pastes, at different concentrations and with different particle sizes. The magnitude of the shearing stress, however, varied with the parameters mentioned. The behaviour shown in Figure 24A is interpreted as proof of yielding. Similar behaviour has recently been reported for peanut butter during creep tests (Citerne et al., 2001).

It is interesting to compare this curve with the more common flow curve, shown in Figure 24B, where the grey lines represent the intervals of shear rates limiting the different rheological responses (a, b, c). Considering that the suspensions deform elastically below the yield value, as stated above, it seems uncertain whether the zero-shear viscosity in the flow curves really exists for this type of suspension. The shear rates measured in this region may instead be interpreted as a local rearrangement of the network structure, i.e. elastic deformation, rather than flow (Macosko, 1994).

39

Moreover, the flow curve shows a discontinuity in the shear rate interval between 10^{-1} and 10^{0} s^{-1}, which corresponds to a sudden increase in shear rates over time in the creep test. Similar discontinuities in the flow curves of concentrated suspensions and food dispersions have been attributed to causes such as structural breakage or slip phenomenon (De Kee et al., 1983; Tiziani & Vodovotz, 2005; Qiu & Rao, 1989). Tomato suspensions are likely to exhibit slip at the wall, and this may be the case here.

The magnitude of the yield stress increased after homogenisation, for a given water insoluble solids (**Papers I** and **II,** Fig. 25A), and was significantly higher in HB than in CB pastes (**Paper IV**), as reported previously by others. In the monodisperse colloidal suspensions studied by Buscall et al. (1987), the yield stress increased with decreasing particle size at a given volume fraction of particles (Fig. 25B), as was also observed in the present work. Upon homogenisation, the nature of the network changes and the bonds of the network probably increase in number and strength. Buscall et al. (1987) found that about 40% of the bonds may already be broken prior to yielding.
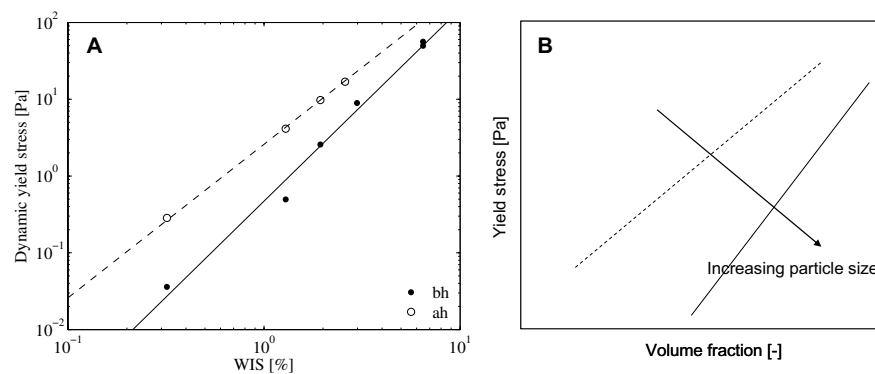
Figure 25. A) Yield stress as a function of the concentration (WIS) for HB suspensions, before (●) and after (○) homogenisation. (Adapted from **Paper II**.) B) Interpretation of the results of Buscall et al. (1987).

5.1.3 Time dependency

In time-independent materials, the rheological response is instantaneous, whereas in time-dependent materials, the response to the applied mechanical forces is delayed. Constant shear forces can induce changes in the aggregate structure by altering the interaction forces between the particles (Macosko, 1994), which gives rise to gradual

changes in viscosity. Materials are then classified as thixotropic, if their viscosity decreases as a function of time at a constant applied shear rate, or as rheopectic, if the viscosity increases with time, at a constant applied shear rate.

The changes in the microstructure of the suspensions induced by prolonged shearing, include the breakage of the network into smaller flocs. The subsequent recovery of the initial structure can take an extremely long time, and might not take place through the same intermediate states, giving rise to a complex shear history dependence (Macosko, 1994). The forces governing the time-dependent behaviour arise from the balance between the structural breakdown due to shearing forces, and the build-up due to attractive forces during collisions and Brownian motion (Barnes, 1997). In flocculated systems, thixotropy can also result from the orientation of the fibres in the flow direction. Marti et al. (2005) studied the relation between the time-dependent rheological behaviour and the well-defined structure of a mixture of spheres and fibres in a suspension. They found that these particulate suspensions exhibited rheopectic behaviour at short times and thixotropic behaviour at longer times, the former being very pronounced only when anisotropic fibres were present in the suspension.

The rheological behaviour of concentrated suspensions, including foodstuffs, is influenced by the shear history of the sample (De Kee et al., 1983, Cheng, 1986), and already in 1965, Harper and Sahrigi (1965) found that tomato concentrates exhibited time dependency. De Kee et al. (1983) studied the behaviour of tomato juice following prolonged shearing, and found that it exhibited rheopectic behaviour (time-thickening) at short times, and thixotropic behaviour (time-thinning) at longer times. This behaviour has also recently been observed by others (Tiziani & Vodovotz, 2005). Detailed reviews on thixotropy can be found elsewhere (Mewis, 1979; Barnes, 1997).

The second part of the study described in **Paper II** was concerned with the time-dependent rheological properties of tomato suspensions subjected to low and high shear stresses, taking into account the effect of particle size and concentration.

Time dependency at low deformations

At stresses just beyond the yield stress, the transient viscosity is found to increase and reaches a steady-state value at rather low deformations, $\gamma < 5$, in non-homogenised systems. In homogenised suspensions, the increase in viscosity is more pronounced, and a peak is observed at high concentrations. The steady-state viscosity is achieved at relatively larger deformations, i.e. $\gamma > 10$ (Fig. 26) for most concentrations.

Figure 26. Transient viscosity as a function of the deformation in HB paste, A) before homogenisation, and B) after homogenisation, at different concentrations: 50 (long dashed), 40 (dotted), 30 (dash-dotted) and 20 (solid) % (higher viscosity corresponds to higher concentration). (Adapted from **Paper II**.)

This initial rheopectic behaviour of the material is characteristic of fibre suspensions and has been attributed to a combination of causes. According to Marti et al. (2005) these may be: i) the formation of slip layers leading to very low start-up viscosity readings, ii) the hindrance of fibre rotation by neighbouring fibres, and iii) the delayed response of the sheared material due to the elastic properties of the fibre network.

In the present work, it is suggested that the orientation of the fibres in laminar flow can be described geometrically, following Jeffery orbitals (Jeffery, 1922)

$$\tan \theta = a_p \tan \left(\frac{\dot{\gamma} t}{a_p + 1/a_p} \right) + \tan \theta_0 . \qquad (10)$$

In the tomato suspensions studied here (Fig. 26), the steady-state viscosity is normally reached at $\gamma < 5$ before homogenisation and at $\gamma > 10$ after homogenisation, which

would correspond to aspects ratios of the order of 1 to 3 and 10 to 30, respectively. These aspect ratios are found to be in qualitative agreement with those obtained using microscopy, reported in Section 3.3 and **Paper III**, for non-homogenised suspensions with an aspect ratio of ~1.5 while the flocs formed after homogenisation and subsequent shearing had a value of a_p of ~10.

Time dependency at large deformations ($\sigma >> \sigma_y$)

Finally, the behaviour of tomato suspensions at large deformations was studied (Fig. 27). Before homogenisation, the transient viscosity seems to level off at a steady-state value, whereas that of homogenised suspensions tends to decrease gradually, even at very large deformations. In the first case, the system seems to become stable, i.e. time-independent. In the second case, the constant decrease in viscosity at large deformations indicates particle rearrangement (i.e. instability of the system), which is suggested to be caused by flocculation. As indicated by microscopy (Section 3.3), when the system is subjected to shearing, the network is gradually disrupted into apparent aggregates, consisting of densely packed particles. These results suggest that homogenisation increases the susceptibility of the structured suspensions to disrupt into smaller aggregates/flocs under shear.
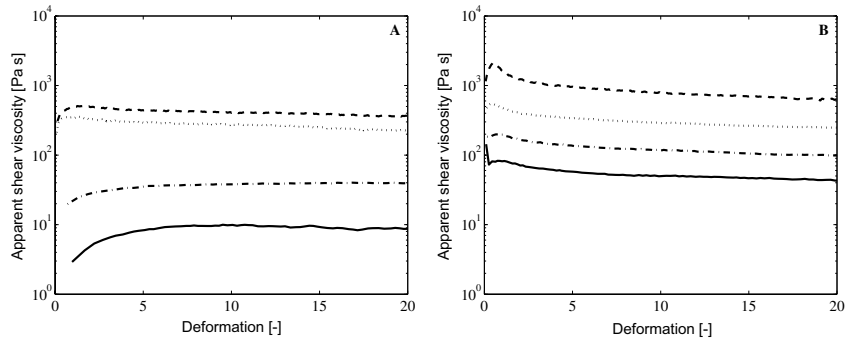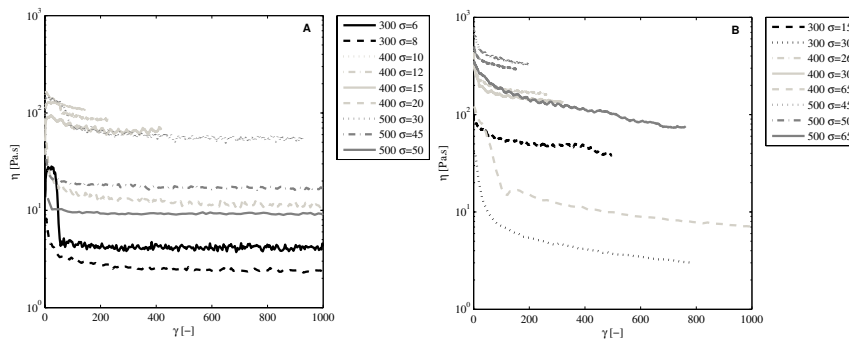

Figure 27. Transient viscosity as a function of the deformation in HB paste, A) before homogenisation, and B) after homogenisation, at different concentrations 500, 400, 300 and 200 g/kg (see legend). The different stresses used are indicated in the legend in Pa. Adapted from **Paper II**.

Combining the information discussed here, with the microscopic images, suggests that the presence of fine particles, caused by homogenisation of the tomato suspensions, plays a major role in determining the time-dependent behaviour of these suspensions (Fig. 28). Yielding of homogenised suspensions requires higher stresses magnitudes or, in other words, the strength of the network is enhanced by homogenisation, and more bonds must be broken before the system overcomes the yield stress and begins to flow. It is interesting to note that about 40% of the bonds in the structure may be broken just prior to yield (Buscall et al., 1987). When applying relatively low shear stress ($\sigma \sim \sigma_y$), a rheopectic response is seen, which might be related in part to rearrangement of the particles, and in part to a delay in the response due to the remaining elastic properties of the network. At these low stresses the system seems to reach an apparent steady-state viscosity after times of about 30 min. It is however not possible to exclude further rearrangements of the particles if a longer time frame is considered. Finally, prolonged and intense shearing gives rise to the formation of flocs of densely packed particles. The illustrations on the left side of the figure (Fig. 28), before shearing, would correspond to the images in Figure 12 (non-sheared, H0, H3), whereas the right side of the drawing instead corresponds to the images in Figure 12 (sheared, H0, H3).
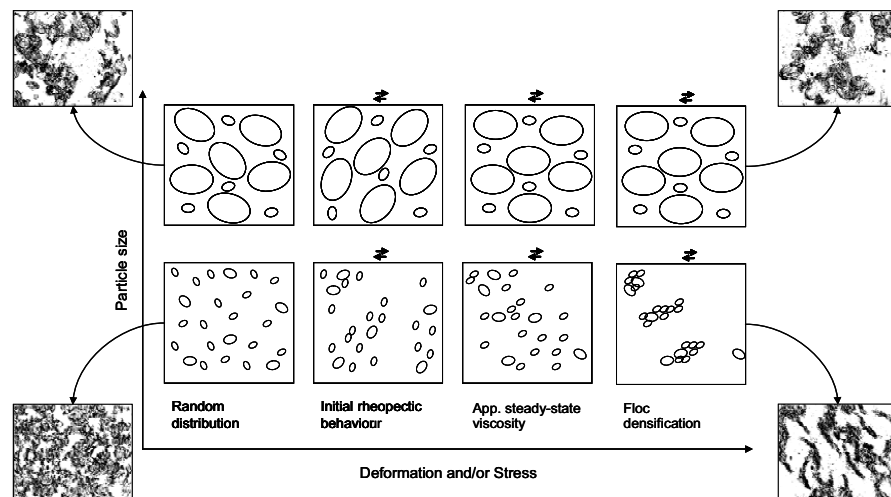

Figure 28. Illustration of the behaviour of concentrated suspensions with predominantly coarse or predominantly fine particle, upon the application of prolonged shear at small and large deformations.

5.2 Measurement systems

There are a large number of instruments and geometries capable of measuring the rheological properties of fluids, and their different principles, applications and limitations have been covered in a number of books (e.g. Macosko, 1994; Steffe, 1996). In this work, a tube viscometer with three diameters, and a rotational rheometer with three geometries: concentric cylinder, vane and vane-vane were used. Their principles and main governing equations will be described in the following sections.

5.2.1   Rotational rheometers

The concentric cylinder rheometer was developed at the end of the 19th century by Couette. Today most instruments have a basic geometry that consists of a static cup, and an inner rotating cylinder. The equations relating the shear stress to the torque measurements (M_i), and the shear rate to the angular velocity (Ω) are obtained under the assumptions of steady, laminar, isothermal flow, and with no end or gravity effects. The shear stress and the shear rate are defined as follows:

$$\sigma_{r\theta} = \frac{M_i}{2\pi R_i^2 h} \tag{11}$$

$$\dot{\gamma} = \frac{\Omega(R_O + R_i)/2}{R_O - R_i} \tag{12}$$

where R_i and R_o are the radius of the bob and cup, respectively and h is the height of the bob. Common problems encountered in the use of this geometry are end effects, disturbance of the flow by the presence of particles, wide gaps with a shear rate gradient across the gap, and wall slip.

Modifications to the concentric cylinder geometry are useful when studying fluids containing large particles. These modifications can also prevent slippage at the walls to some extent. The vane geometry is known to reduce or eliminate these two problems (Nguyen and Boger, 1992; Barnes, 1999), and simultaneously minimises the amount of disturbance when it is introduced into a complex fluid. The use of vane geometry in the yield stress measurements of food suspensions has become increasingly popular (Yoo, et al., 1995), and recently its use has been extended to the measurement of other rheological

properties (Krulis & Rohm, 2004). A detailed review of the use of the vane geometry is available elsewhere (Barnes & Nguyen, 2001).

Geometries used for all measurements reported in Papers I-IV

A four-blade vane was constructed for measuring the rheological properties of concentrated tomato suspensions in a smooth cup (**Paper I-IV**). A vane cup was also constructed and this was only used in the study described in **Paper IV** (Fig. 29).
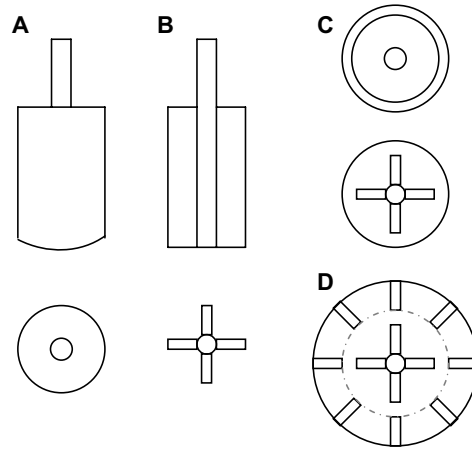
Figure 29. Schematic illustrations of: A) a concentric cylinder, B) the vane geometry, C) the previous geometries inside the smooth cup, and D) the vane geometry in the vane cup.

The stress and shear rate calculations are based on the analysis carried out by Barnes and Nguyen (2001).

$$\sigma = M\sigma_f = M\frac{1}{2\pi R_i^3}\left(\frac{h}{R_i}+\frac{2}{3}\right)^{-1} \tag{13}$$

$$\dot{\gamma} = \Omega\gamma_f = \Omega\frac{2R_o^2}{R_o^2-R_i^2}\,. \tag{14}$$

The conversion factors (σ_f, γ_f) from angular velocity (Ω) to shear rate ($\dot{\gamma}$), and from torque (M) to shear stress (σ), depend on the geometry of the vane. These equations are derived assuming that the material entrapped between the blades of the vane forms a virtual inner cylinder. In fact, the vane does not form a "perfect" cylinder and, therefore,

the calculated conversion factors have to be slightly corrected. For this correction, Newtonian syrup with a defined viscosity of 7.1 Pa s at 20°C was measured using both the conventional concentric cylinder (d =25 mm) and the vane.

The vane cup was employed as it was thought that the slippage at the outer wall could be avoided. It was constructed such that the radius of the virtual cylinder formed by the blades in the cup, corresponded to that of the smooth cylinder (Fig. 29). The calibration procedure followed was the same as in the vane geometry, and the conversion factors were found to be equal (Table 6).

A tomato paste suspension was measured in the concentric cylinder (CC), the vane+smooth cup (V) and vane+vane cup (VV), to investigate their performance on non-Newtonian suspensions. The results were as expected (Fig. 30). The concentric cylinder gave lower viscosity values probably due to slippage at the wall, while the viscosity obtained with the vane+smooth cup and vane+vane cup coincided over a large range of shear rates.

Table 6. Main characteristics of the geometries used in the rheometer.

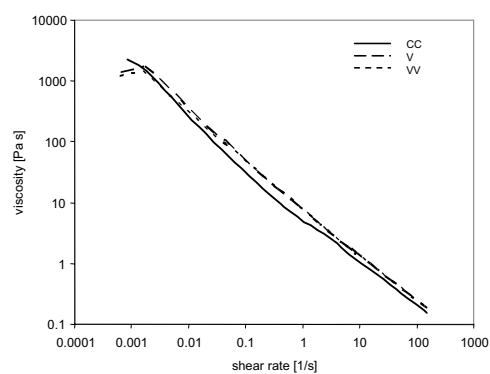| Type of geometry	σ_f Pa/Nm	γ_f 1/s	R_i mm	R_o mm	h mm	Gap mm
Concentric cylinder	24998	12.25	12.5	13.6	37.5	1.1
Vane / Vane-Vane	24560	4.7	10.5	13.6	45.0	3.1

Figure 30. Comparison between viscosity measurements performed in a concentric cylinder, with the vane geometry and smooth cup, and vane geometry in a vane cup on 30% tomato paste suspension.

In fact, earlier studies have already suggested that the behaviour of tomato concentrates at low shear rates may be strongly influenced by secondary effects such as yield phenomena, time dependency and wall effects, i.e. slippage (Harper and El Sahrigi, 1965). These effects are related to each other (Windhab, 1988), and they all complicate the measurement of the rheological properties in common rotational rheometers. The remaining part of this thesis is devoted to discussing common problems that occur during the determination of the flow behaviour of concentrated suspensions.

5.2.2   Tube viscometers

Tube or capillary viscometers were developed in mid 19th century to measure the viscosity of fluids under laminar conditions. Advances in the field of small-bore tubing, which allowed precise determination of the tube diameter, were key to the development of this technique (Macosko, 1994). This was important because the viscosity depends on the tube radius to the power four.

Compared with rotational rheometers, tube viscometers have the advantage of being able to measure particulate suspensions, i.e. with large particles, in an interval of shear rates that is relevant for food processing, i.e. $100 < \dot{\gamma} < 1000$ s^{-1}. This is sometimes difficult to achieved in rotational rheometers, as discussed above. Some drawbacks of using tube viscometers are, however, the fact that they require large floor space and large amounts of sample.

Tube viscometers employ a pressure-driven flow, which creates a velocity gradient through the tube, with the maximum velocity at the centre of the pipe. The pressure drop and volumetric flow rate are measured and converted to shear stress and shear rate, respectively. The main assumptions in the derivation of rheological data for incompressible fluids are:

- fully developed, steady-state, laminar flow in the pipe,
- velocity only in the length direction (x), and
- no wall slip, the velocity at the wall is zero, $v_x(R)=0$.

The shear stress at the wall (σ_w) can be derived from a force balance over a cylindrical fluid element giving Eq. 15,

$$\sigma_w = \frac{RdP}{2L} \tag{15}$$

where R is the radius of the tube and dP is the pressure drop over a distance L. The volumetric flow rate (Q) can be defined as:

$$Q = 2\pi \int_0^R v_x(r)rdr = \pi \int_0^{R^2} v_x(r)dr^2 \text{ , or} \tag{16a}$$

$$Q = \frac{\pi R^3}{\sigma_w^3} \int_0^{\sigma_w} \sigma^2 f(\sigma)d\sigma . \tag{16b}$$

where $v_x(r)$ is the velocity profile over the tube radius. The solution of Equation 16b depends on the fluid model $\dot{\gamma} = f(\sigma)$ considered, and can be performed analytically for some simple models (Steffe, 1996). In Table 7, some of the analytical solutions are summarized.

Table 7. Analytical solution of Equation 16b, for some common fluid models.

Fluid model	$\dot{\gamma} = f(\sigma)$	Analytical solution
Newtonian	σ/μ	$Q = \dfrac{\pi R^4 dP}{8L\mu}$
Power law	$(\sigma/K)^{1/n}$	$Q = \pi\left(\dfrac{dP}{2LK}\right)^{1/n}\left(\dfrac{n}{3n+1}\right)R^{(3n+1)/n}$
Herschel-Bulkley	$\left(\dfrac{\sigma-\sigma_y}{K}\right)^{1/n}$	$Q = \dfrac{\pi}{K^{1/n}}\left(\dfrac{2L}{dP}\right)^3\left[\dfrac{\sigma_w^2(\sigma_w-\sigma_y)^{1+1/n}}{1+1/n} - \dfrac{2\sigma_w(\sigma_w-\sigma_y)^{2+1/n}}{(1+1/n)(2+1/n)} + \dfrac{2(\sigma_w-\sigma_y)^{3+1/n}}{(1+1/n)(2+1/n)(3+1/n)}\right]$

Equation 16a reduces to the well-known Weissenberg-Rabinowitsch equation, and the solution depends on the derivative of the logarithm of the flow rate and the wall shear stress.

$$\dot{\gamma} = -\frac{dv_x}{dr}\bigg|_{\sigma_w} = \frac{Q}{\pi R^3}\left[3 + \frac{d\ln Q}{d\ln\sigma_w}\right] \tag{17}$$

49

The problem of generating shear rate and shear stress data from capillary data (i.e. from pressure drop and volumetric flow) is formulated, in Equation 16b, as a Volterra integral equation of the first kind, and the solution may not be unique and may not depend continuously on the data. This is known as an ill-posed inverse problem, and its mathematical treatment can be complicated. Common non-linear methods are difficult to apply because many local minima may exist and the result is thus very dependent on the initial conditions.

Tube viscometers are useful for obtaining viscosity data for concentrated suspensions at high shear rates, which might be difficult to achieve in other kinds of equipment. However, some problems can be encountered in tube viscometer measurements:
a) entrance effects, b) compression of the material and pressure dependence, c) deterioration of the material by prolonged shearing, and d) wall slip. Data corrections are often required and the description of some of these corrections can be found elsewhere (Steffe, 1996).

Tube viscometer set-up used (Paper IV)

A tube viscometer consisting of three pipes with different diameters, d_0 = 20, 25, and 38 mm was constructed. The pressure drop was determined over a straight section of the pipe with a length of L = 3.42 m. The pressure drop per unit length (dP/L) was checked to be constant at a given flow rate, by estimating the pressure drop between points 1 and 3 (Fig. 31), which should be equal to the pressure at point 1 $dP_{1-3} = P_3 - P_1 = P_1$, and hence the entrance pressure losses were assumed to be negligible.
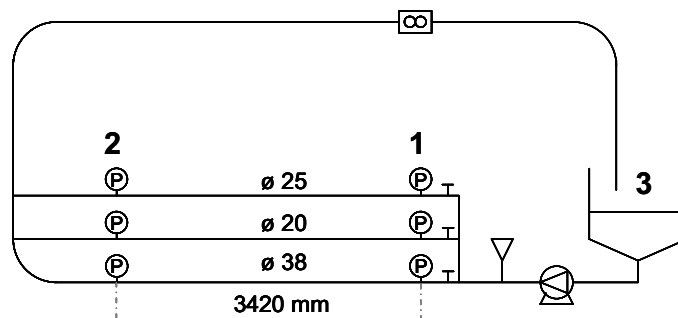

Figure 31. Schematic diagram of the experimental set-up for the determination of rheological properties in tube flow.

The system was first calibrated with several Newtonian syrups with different viscosities, and was found to perform very accurately (Fig. 32).
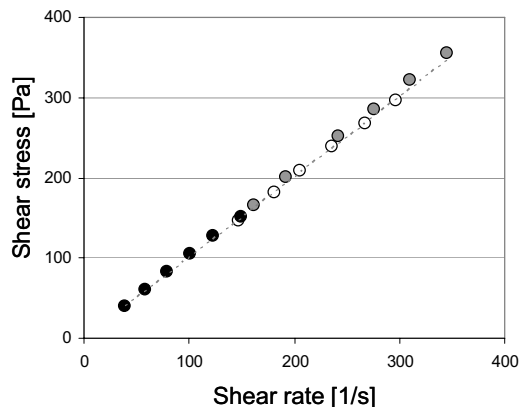

Figure 32. Shear stress as a function of the shear rate for 71.8°Brix syrup at 19.6°C, with a Newtonian viscosity of 1 Pa s, measured in tubes of different diameters: 20, 25 and 38 mm (◐, ○ and ●, respectively). The dotted line represents the "real" flow curve, measured in a rotational rheometer using concentric cylinders.

5.3 Quantification of apparent wall slip and determination of flow behaviour in the tube viscometer

The flow behaviour of complex suspensions in a tube viscometer may be affected by apparent wall slip. The apparent slip is caused by the migration of the liquid phase towards the fluid-wall interface (Martin & Wilson, 2005), because the particles can not physically occupy the space adjacent to the wall (Kalyon, 2005). This leads to the formation of a thin layer of less concentrated suspension at the wall, with a thickness of the same order of magnitude as the particle size (Yilmazer & Kalyon, 1989). The slip layer has a lower viscosity than the bulk fluid and distorts the velocity profile in the tube (Fig. 33).

Apparent wall slip has been reported for food products such as tomato paste, apple sauce, ketchup and mustard (Dervisoglu & Kokini, 1986). Tomato concentrates at concentrations of 12 °Brix exhibited slip velocities from 2 to 12 cm/s at shear wall stresses below 20 Pa, and the flow rate governed by the slip was as high as 80% of the

total flow (Lee et al., 2002). The occurrence of slip at the wall results in a lower resistance to shear, which gives rise to the underestimation of the fluid viscosity. This becomes a major problem for food engineers when designing industrial equipment based on rheological data obtained in the presence of slip.
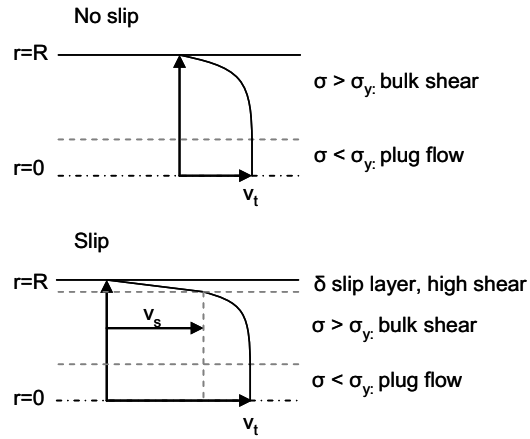
Figure 33. Velocity profiles in a tube viscometer, for a fluid with yield stress, with no slip and under wall slip conditions.

5.3.1 The classical Mooney method

Mooney (1931) suggested a method for the correction of wall slip based on the assumption that the slip velocity (v_s) is a function only of the wall shear stress,

$$v_s = \beta(\sigma_w)\sigma_w \tag{18}$$

where β is the slip coefficient. The measured flow (Q_m) can be divided into two parts, one due to the slip velocity (Q_s), and the other due to the shear rate in the fluid (Q_{ws}),

$$Q_m = Q_s + Q_{ws} = v_s \pi R^2 + \frac{\pi R^3}{\sigma_w^3} \int_{\sigma_y}^{\sigma_w} \sigma^2 f(\sigma)d\sigma \tag{19}$$

By combining Equations 18 and 19, and dividing by $1/\sigma_w \pi R^3$, he obtained,

$$\frac{Q_m}{\sigma_w \pi R^3} = \frac{\beta}{R} + \frac{1}{\sigma_w^4} \int_{\sigma_y}^{\sigma_w} \sigma^2 f(\sigma) d\sigma \qquad (20)$$

Generally, the Mooney graphical correction requires measurements in tubes of at least three diameters. At a constant wall shear stress, the slope of a plot of $Q_m/\sigma_w \pi R^3$ against $1/R$ is equal to the slip coefficient β. In practice, it is difficult to obtain data in the tube viscometer at the same wall shear stress, and the rheological behaviour of the suspensions must be interpolated and/or extrapolated (Fig. 34A).
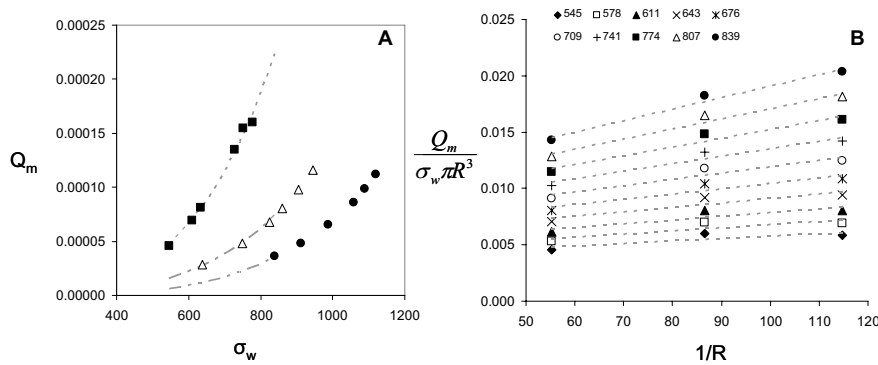
Figure 34. Example of the Mooney method for slip correction. A) Tube viscometer data from HB tomato paste, obtained at different tube diameters 20 mm (●),25 mm (Δ) and 38 mm (■). The grey lines represent the extrapolation made to obtain the Mooney plot shown in B) $Q_m/\sigma_w \pi R^3$ as a function of 1/R., the extrapolated wall shear stresses are given in the legend in Pa. (Adapted from **Paper IV**.)

The dependence of the slip velocity on the wall shear stress was obtained for HB tomato paste (100%) following the Mooney procedure: $v_s = 3 \cdot 10^{-15} \sigma_w^{4.6}$, and the result was of the same order of magnitude as other published data (Kokini & Dervisoglu, 1990). However, the Mooney method has been found to fail in some fluids, especially in pastes, when the Mooney plot does not give linear slopes (Martin & Wilson, 2005), or when the slope becomes negative. This might arise from the required extrapolation or interpolation of data, as well as from the inherent poor reproducibility of concentrated suspensions. This problem was encountered when analysing the CB paste (**Paper IV**).

5.3.2   A numerical method of quantifying slip and flow behaviour

Recently, Yeow et al. (2000) developed a new method to extract rheological data from tube viscometers in yield stress fluids, using inverse problem solution techniques and Tikhonov regularization. It has been reported to work on fruit purees with no slip (Yeow et al., 2001). Later, the method was extended to cope with the presence of wall slip (Yeow et al., 2003), based on the Mooney analysis, with the advantage that it uses the whole set of data without any need for extrapolation, and does not require the assumption of any rheological or slip model. Martin and Wilson (2005) applied this numerical method to published data for polymers, foams and pastes, and found that the method worked well on polymers and foams, but not as well on pastes. The same numerical method was applied in the present work (**Paper IV)** in order to quantify the wall slip and to obtain the flow behaviour of dried potato fibres suspended in low- and high-viscosity syrup, as well as in tomato paste suspensions made from hot and cold break pastes.

The numerical method used will be referred to as the Mooney-Tikhonov method. The Mooney equation (Eq. 20) can also be written in the form of apparent shear rate $\dot{\gamma}_a^c$ as,

$$\dot{\gamma}_a^c = \left(\frac{4Q_m}{\pi R^3}\right)^c = \frac{4v_s(\sigma_w)}{R} + \frac{4}{\sigma_w^3}\int_{\sigma_y}^{\sigma_w}\dot{\gamma}(\sigma)\sigma^2 d\sigma . \tag{21}$$

The first part is the contribution of the wall slip to the shear rate, and the second part is that of the shear flow. To apply the Mooney-Tikhonov method, the interval between the minimum and maximum values of σ_w in the set of data was divided into N_j uniformly spaced points, and the unknown slip velocities at these points were represented by a vector $\mathbf{v_s} = [v_1, v_2, \ldots v_{Nj}]$. In the same way, the integration interval (σ_y to σ_w) in Equation 21 was divided into N_k uniformly spaced points, and the unknown shear rates at these points were represented by the vector $\dot{\gamma} = [\dot{\gamma}_1, \dot{\gamma}_2, \ldots \dot{\gamma}_{N_k}]$. The precision of the solution was evaluated by the sum of the squares of the deviation between the calculated solution (superscript c) and the experimental measured data (superscript m),

$$S_1 = \sum_{i=1}^{N_p} \delta_i^2 = \sum \left[\frac{\dot{\gamma}_{a,i}^m - \dot{\gamma}_{a,i}^c}{\dot{\gamma}_{a,i}^m} \right]^2 \qquad (22)$$

and to ensure that the shear rate $\dot{\gamma}(\sigma)$ and the slip velocity $v_s(\sigma)$ functions varied smoothly with the local stress, the sum of the squares of the second derivatives of these two functions, at the internal discretization points, was minimised,

$$S_2 = \frac{4}{R_{min}} \sum_{p=2}^{N_{j-1}} \left(\frac{d^2 v_s}{d\sigma_w^2} \right)_p + \sum_{q=2}^{N_{k-1}} \left(\frac{d^2 \dot{\gamma}}{d\sigma^2} \right)_q . \qquad (23)$$

Tikhonov regularization minimises a linear combination of these two quantities,

$$R = S_1 + \lambda S_2 , \qquad (24)$$

where λ is an adjustable numerical factor. For example, a large value of λ favours the smoothness conditions over the goodness of the fit. The condition that the shear rate is zero at the yield stress should also be satisfied, and is solved iteratively for $\dot{\gamma}(\sigma_y) = 0$.

Comparison between the classical Mooney method and the Mooney-Tikhonov method

Paper IV describes a study on the flow behaviour of dried fibre suspensions exhibiting liquid-like behaviour (G′<G″), and tomato paste suspensions exhibiting solid-like behaviour (G′>G″). The uncorrected tube viscometer data, in the form of wall shear stress as a function of the apparent Newtonian shear rate, are shown in Figure 35.

It was first determined whether slip occurred by testing if the mean rheological data was different in different tube diameters, using a t-test. When the t-test was significant, slippage was assumed to be present (cf. predicted behaviour in Table 8). The solutions obtained by the application of the classical Mooney method, i.e. graphical procedure, were then compared with the approximation given by the Mooney-Tikhonov numerical method. The results are summarised in Table 8.
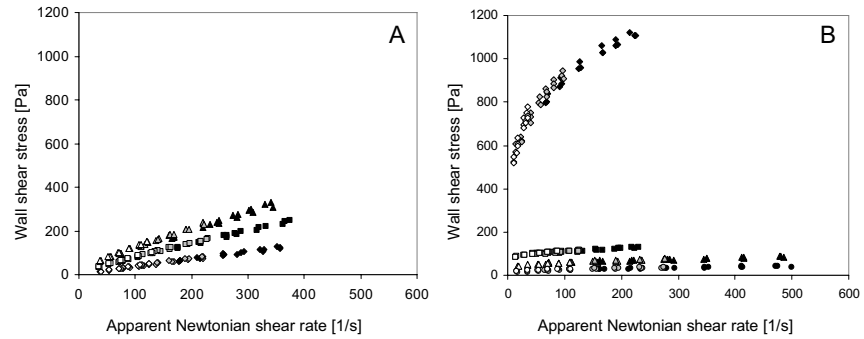
Figure 35. Uncorrected tube viscometer data expressed as wall shear stress plotted against apparent Newtonian shear rate for: A) dried potato fibre at different concentrations: 4.5 (◊), 5.6 (□) and 6.5% (Δ), suspended in low-viscosity syrup (68 mPa s), and B) HB tomato paste suspensions, at different concentrations: 100 (◊), 50 (□) 40 (Δ) and 30% (○). The data were obtained with three tube diameters: 20, 25 and 38 mm, corresponding to empty, grey and black symbols, respectively. Three replicate measurements are shown. (Adapted from **Paper IV**.)

In the dried potato suspensions, where no slip or almost no slip conditions were expected, the classical Mooney method tended to give low Q_s/Q_m values, in most cases, with the contribution of slip gradually decreasing with increasing shear stress. The Mooney-Tikhonov procedure gave somewhat higher Q_s/Q_m ratios for the highly viscous solution, and negative values of slip velocity for the low viscosity dried fibre suspension. The behaviour of the Q_s/Q_m ratio predicted by the numerical method is not gradual, but usually showed a maximum at low stresses and decreased towards higher stresses (↑↓). The negative values in the slip velocity give rise to too high calculated shear rate values, and they tend to appear when no slip was present.

The Mooney method seems not to apply in most of the tomato paste suspensions, as it results either in non-linear slopes or unrealistic slip flow, Q_s/Q_m >100%. These problems could arise from the data extrapolation or from the inherently poor reproducibility of the data. The error between repeated measurements was found to be acceptable, usually below 10%, but in some cases it was as high as 17%. Such relatively high error values are often reported for this type of system, as explained in Section 5.1. There is, however, a notable exception where the classical Mooney method gave good results, i.e. in HB tomato paste at 50 and 100% concentration (the latter shown in Fig. 34). The numerical procedure gave negative slip values at almost all concentrations, except for the pure

tomato paste samples and the 50% CB suspension. The Mooney-Tikhonov method tends to underestimate the slip velocity at high shear rates, resulting in too high calculated shear rates.

Table 8. Estimation of wall slip using the classical Mooney graphical approach and the numerical Mooney-Tikhonov method in four series of suspensions: dried potato fibres in high viscous syrup (A) and low viscous syrup (B) and HB and CB tomato paste at different concentrations. The predicted behaviour was determined by comparing the mean rheological data between different pipe diameters using a T-test ($p<0.05$). The calculated interval for the Q_s/Q_m ratio is given. (Adapted from **Paper IV**.)

	Predicted behaviour	Classical Mooney		Mooney-Tikhonov		
	t-test	Q_s/Q_t (%)	f(σ)[b]	Q_s/Q_t (%)	f(σ)[c]	
Fibre suspension						
A-4.5 %	No slip	1.4 – 14 [a]	↑	5 – 23	↓	*
A-5.6 %	No slip	6.9 – 15 [a]	→	3 – 43	↑↓	
A-6.5 %	No slip	6.3 – 20 [a]	↓	0 – 15	↑↓	
B-4.5 %	Slip	8 – 27	↓	$v_s<0$	x	*
B-5.6 %	Slip	0 – 37	↓	$v_s<0$	x	*
B-6.5 %	Slip	1 – 65	↓	1 – 17	↓	
Tomato paste						
HB-30 %	Slip	>100	x	$v_s<0$	x	*
HB-40 %	No slip	>100	x	$v_s<0$	x	*
HB-50 %	Slip	7 – 86	↓	$v_s<0$	x	*
HB-100 %	Slip	27 – 69	↑	3 - 88	↑↓	
CB-30 %	Slip	n. l. σ >32 Pa	x	$v_s<0$	x	*
CB-40 %	Slip	n. l. σ >77 Pa	x	$v_s<0$	x	*
CB-50 %	Slip	n. l. σ >130 Pa	x	0 - 23	↓	*
CB-100 %	Slip	>100 x	x	3 - 119	↑↓	*

[a] Only two diameters were used

[b] variation of Q_s/Q_t as a function of σ. ↑ increases, → no variation, ↓ decreases, x no physical meaning

n.l. non linear

* too high calculated shear rates

Since reasonable results were obtained for the 100% HB tomato paste using both the classical Mooney and the numerical Mooney-Tikhonov methods, the corrected shear rate values calculated using both methods are compared in Figure 36. Note that the former method predicts much lower shear rates in the fluid than the measured ones, e.g. at $\sigma_w \sim 1100$ Pa, the uncorrected shear rate was slightly more than 200 s^{-1}, whereas after slip

correction it is only ~50 s^{-1}. The too high shear rates calculated with the Mooney-Tikhonov method are obvious in the flow curve (Fig. 36), as the shear rates are larger than the measured ones.
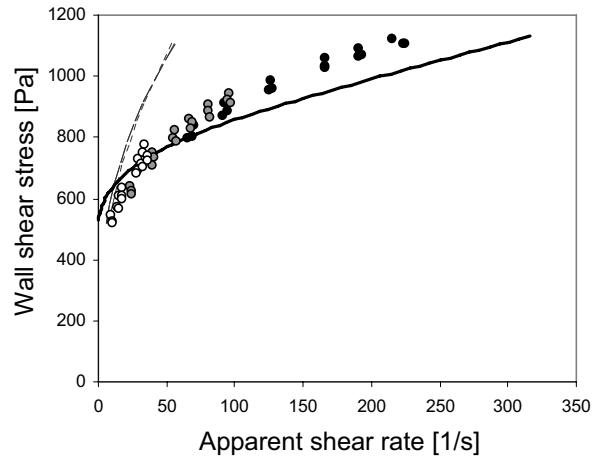

Figure 36. Uncorrected tube viscometer data expressed as wall shear stress plotted against the apparent Newtonian shear for different tube diameters (20 (●), 25 (◉) and 38 mm (○), and data after correction for slip using the classical Mooney (dashed line) and the Mooney-Tikhonov methods (heavy line).

Comparison between data obtained in the tube viscometer and rotational rheometer

A comparison between the tube viscometer data and rheological data (measured in a rotational rheometer using different geometries) might give some insight into the "real" flow and slip behaviour of these suspensions. In the rotational rheometer, different geometries were used to obtain different degrees of slippage on the rheometer walls (Fig. 29). The concentric cylinders had smooth walls and the tomato paste was expected to exhibit wall slip. The vane was expected to prevent slip on the inner wall of the cylinder, while slip might occur on the outer wall (i.e. at the cup wall) when high stresses were applied (see Section 5.1.2). The vane-vane geometry was constructed to prevent slip on the outer wall.

In Figure 37, the flow curves of 100% HB tomato paste, expressed as shear stress as a function of the shear rate, are shown for each of the measurement systems used. The

58

flow curves corrected for slip by the classical Mooney and Mooney-Tikhonov methods are also included. It is interesting to note that the tube viscometer data corrected for slip by the classical Mooney method correspond well with the rheological data obtained using the vane and vane-vane geometries. The concentric cylinders with smooth walls gave similar values at very low shear rates, $\dot{\gamma} < 2.5$ s^{-1}, but the values deviated considerably at higher shear rates, giving values even lower than those obtained from the uncorrected data in the tube viscometer, which seems to indicate that the slip in concentric cylinders is substantially greater than in the tube viscometer.
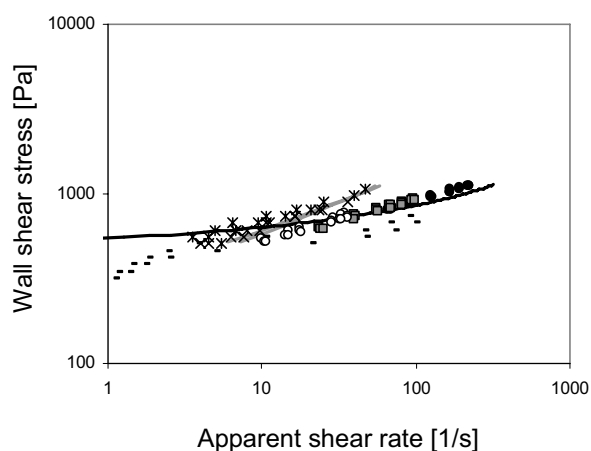

Figure 37. The flow curves, expressed as shear stress as a function of the shear rate, for 100% HB tomato paste obtained using different systems: tube viscometer with different diameters (20 (●), 25 (◎) and 38 mm (○), uncorrected data), and a rotational rheometer using different geometries: concentric cylinders (-), vane (x), vane-vane (*). The classical Mooney correction (▬) and the Mooney-Tikhonov (▬) correction are included.

5.4 Comparison of dynamic rheology and flow behaviour –The Cox-Merz rule

In highly concentrated suspensions, dynamic oscillatory measurements are easier to perform experimentally (Doraiswamy et al., 1991), and show better reproducibility, than steady shear measurements. Moreover, dynamic experiments on food materials such as mayonnaise, which often exhibit apparent wall slip in steady shear, have been found to give true material properties when small strain amplitudes <1% were used, with no detectable wall slip distorting the results (Plucinski et al., 1998). In 1958, Cox and Merz

discovered an astonishingly simple and empirical relationship between the steady shear viscosity $\eta(\dot{\gamma})$ and the complex viscosity $\eta*(\omega)$,

$$\left|\eta*(\omega)\right| = \eta(\dot{\gamma} = \omega) . \qquad (25)$$

The Cox-Merz rule holds for simple polymeric fluids, but is not reliable for more complex and structured fluids such as crystalline polymers, concentrated suspensions or gels (Larsson, 1999). Bistany and Kokini (1983) reported a lack of validity of this rule for various types of food materials, such as butter, ketchup, margarine and cream cheese, where they found that dynamic and steady shear data could only be superposed by using a shift factor. The same type of shifting was used in data from tomato pastes (Rao & Cooley, 1992), but no theoretical explanation was given. Recently, Muliawan & Hatzikiriakos (2007) investigated cheese at different temperatures, and at low temperatures they observed a shift between dynamic and steady shear data, that tended to disappear when the cheese melted and lost its structure.

Small-amplitude oscillatory measurements tend to preserve the microstructure of the material being tested (see Chapter 4), whereas steady shear measurements can induce changes in the microstructure of the suspensions (see Section 5.1.3), disrupting the network to some extent. This difference in the conservation of the microstructure might explain the lack of agreement between the two types of data in complex structured food materials.

For example, in Figure 35A complex and steady shear viscosities are plotted for a suspension of dried potato fibres in highly viscous syrup. The Cox-Merz rule seems to hold for this set of data. In the case of the 30% tomato suspension (Fig. 35B), however, the complex viscosity is shifted to higher values than those of the steady shear viscosity. The potato suspension exhibits liquid-like behaviour at all frequencies ($G'<G''$) and exhibits no yield stress. The tomato suspensions, on the other hand, exhibit solid-like behaviour over the range of frequencies studied ($G'>G''$), and had a yield stress. Hence, the lack of a network structure in the dried fibre suspensions seems to be a key factor in the validity of the Cox-Merz rule.
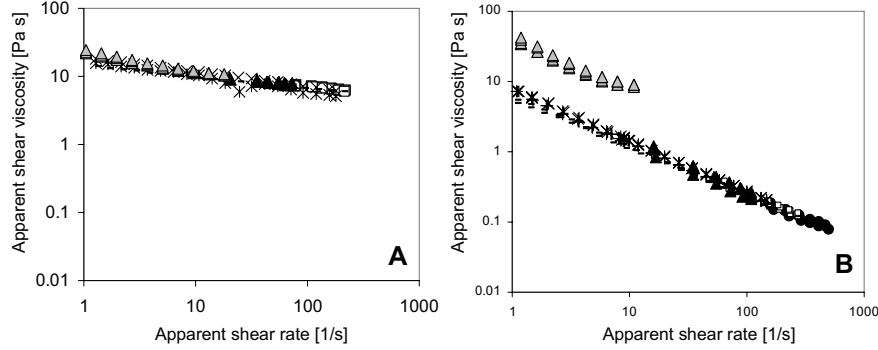
Figure 38. Complex viscosity (△) and steady shear viscosity obtained in a tube viscometer with d=20 (●), 25 (□) and 38 mm (▲), and a rotational rheometer with concentric cylinders (-), vane (x) and vane-vane geometries (*), for: A) 5.6% dried potato fibres suspended in a syrup with viscosity 860 mPa s, and B) a 30% HB tomato suspension. (Adapted from **Paper IV**.)

Some theoretical work has also been devoted to extending the validity of the Cox-Merz rule to concentrated suspensions with negligible yield stress (Gleissle & Hochstein, 2003) and other materials with yield stress (Doraiswamy et al., 1991). The former researchers modified the Cox-Merz rule to give:

$$\frac{|\eta^*(\omega)|}{B(c_v)} = \frac{\eta(B \cdot \dot{\gamma} = \omega)}{B(c_v)} = \eta(\dot{\gamma} = \omega)_{c_v=0} \qquad (26)$$

where B is a shifting factor used to superpose the steady shear (η) and the complex viscosity (η^*) curves at a given concentration (c_v) to the η or η^* curves of the suspending medium (c_v=0). The equation works for situations where the particle-particle interaction is negligible, i.e. the yield stress $\sigma_y \ll \sigma$, and hydrodynamic effects dominate, i.e. relatively high shear rates. However, it might be difficult to apply this procedure to real food systems, such as tomato paste, because the suspending medium is not well defined and is difficult to reproduce in a lab, since it includes a range of soluble materials such as sugars, pectins and proteins, among others. In addition, series of tomato paste concentrations made by dilution in water change the viscosity (Fig. 22) and probably the nature of the suspending medium.

Doraswamy et al. (1991) developed a model that takes into account the elastic and viscous behaviour typical of concentrated suspensions, which led to a modified Cox-

61

Merz rule (Eq. 27), which basically consists of the application of a shift factor to give an "effective shear rate". The equation was, however, only tested at $\dot{\gamma} < 10$ s^{-1},

$$\left| \eta^*(\gamma_m \omega) \right| = \eta(\dot{\gamma} = \gamma_m \omega) \tag{27}$$

where γ_m is the amplitude of oscillating strain.

Comparison between dynamic and steady shear data

The shift factors used to superpose the complex and the steady shear viscosities, in hot and cold break tomato pastes in the concentration interval between 30 and 100% were calculated (**Paper IV)**. The magnitude of the shift factors as a function of the yield stress of the suspensions is given in Figure 39. The reference steady shear viscosity was that measured with the vane-vane geometry, which seems to be free of wall effects (as indicate in Section 5.3.2). The yield stress provides a measure of the structure of the material. Interestingly, the shift factor is found to be about 0.1 for all the suspensions studied, regardless of the concentration or the yield stress of the suspension. These values are somewhat higher than those found in tomato pastes by Rao and Cooley (1992).
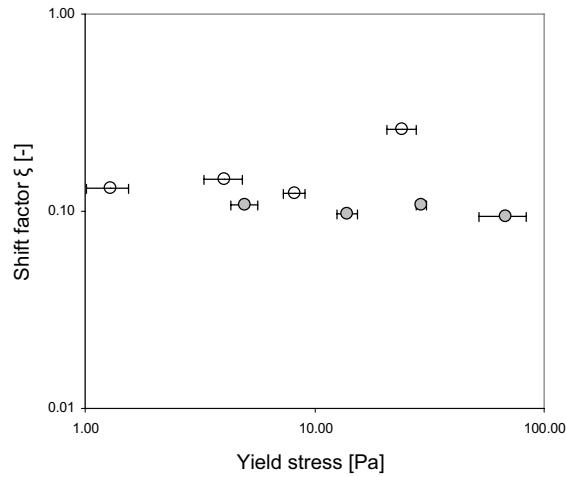
Figure 39. Factor ξ in the modified Cox-Merz rule, $\eta(\dot{\gamma}) = \eta^*(\xi\omega)$, as a function of the yield stress for HB (grey) and CB (empty) tomato paste suspensions at different concentrations.

These shift factors may allow the flow behaviour of the suspensions to be obtained using oscillatory measurements, instead of the more common steady shear measurements, which can be subject to a number of experimental errors. Dynamic data could then be used in food processing design and engineering.

6. Conclusions

Processing of food materials, i.e. homogenisation and subsequent shearing, has a considerable effect on the microstructure of the suspensions formed. These changes are reflected in the textural and rheological characteristics of the processed foods. Structural changes during processing seem to be related to the fractions of fine and coarse particles present in the suspension, the viscosity of the suspending medium, and the concentration.

The presence of fine particles results in marked time-dependent effects, which result from the disruption of the network and the formation of elongated, densely packed flocs of particles upon shearing. These effects are observed as rheopectic behaviour at low deformations, caused by the tendency of the flocs to orient perpendicularly to the flow, and as thixotropic behaviour at large deformations, with extensive disruption of the network, densification of the flocs and an increase in the separation between them.

At high paste concentrations , the rearrangement of particles within the network induced by processing is better reflected by values of the compressed volume fraction than the magnitude of the elastic modulus obtained from small-amplitude oscillatory tests. The relatively poor sensitivity of the elastic modulus to variations in the structure seems to be a consequence of the suspensions being fully packed.

Tomato suspensions exhibit solid-like behaviour ($G'>G''$), at concentrations as low as 10% tomato paste, which indicates the existence of a network, and the suspensions can thus be described as weak gels. These suspensions are characterised by a yield stress, below which the systems are found to deform elastically. Above the yield value, the system begins to flow.

Tube viscometer measurements show that the flow behaviour of tomato paste is substantially influenced by an apparent wall slip, which tends to disappear at lower concentrations. Some difficulties are encountered in the extraction of the rheological data using tube viscometers when wall slip is present.

7. Future Outlook

Basic knowledge on the mechanisms governing structural changes during processing and their relationship to the textural and rheological properties of food suspensions is desirable for the optimisation of industrial food processing. Some insights into these relationships are given in this thesis, but further studies are required.

New approaches are needed, for example, to study and quantify the microstructure. The use of confocal microscopy will allow the localisation of specific structural elements, making it possible to follow their rearrangement in different stages of processing. In addition, the visualisation of the material in three dimensions will be possible. Another new technique, rheo-microscopy, may be useful to observe the structural changes taking place on shearing and, at the same time, relate them to the rheological behaviour.

The process of homogenisation and its capacity to create different networks in the material constitute an enormous field of investigation. The influence of the morphology of the particles and the viscosity of the suspending medium requires further investigation. Moreover, the investigation and understanding of the behaviour of differently homogenised systems upon subsequent shearing are important in order to prevent, or minimise, the loss of textural properties of products made using industrial processes involving homogenisation.

The compressive volume fraction and its sensitivity in detecting small changes in the microstructure of a suspension network should also be studied in greater depth, with the aim of making it possible to measure the porosity of more concentrated suspension networks.

Finally, the formation of slip at the wall in tube viscometers could be directly observed and quantified using techniques such as magnetic resonance imaging (MRI) or ultrasound. The comparison between direct observation of slip and the behaviour predicted by Mooney and Mooney-Tikhonov analysis of the tube viscometer data will give further insights into the "real" flow behaviour of these suspensions.

Acknowledgements

During the four years that it has taken to complete this degree, there have been many people that have contributed in one way or another to this work. I would like to express my gratitude to all of them.

I want to especially thank Eva Tornberg, my supervisor, for giving me the opportunity of doing a PhD, and for her support and encouragement over the years, and her endless enthusiasm about discussing every new result.

I want to thank also Ulf Bolmstedt, my second supervisor, for his positive and supportive attitude over these years and for shearing his experience about the rheology world. Fredrik Innings for good discussions and many comments that have made me think about the results one more time. Also, for his invaluable help in the construction of the rig equipment. Björn Bergenståhl, who gave me some interesting new thoughts for interpreting the results in paper II. Petr Dejmek, always open for discussion, and I really appreciate his help with the Matlab code used in the last paper. I would also like to thank some undergraduate students that have helped me with part of the experimental work, Pernilla Månsson and Peter Jansson.

The following companies are gratefully acknowledged for their financial support of this work: Orkla Foods A/S, Tetra Pak Dairy & Beverage Systems AB and a number of SMEs together with a regional EU fund. The SMEs are Sveriges Stärkelseproducenter, Salico AB, Mariannes Farm AB, Kiviks Musteri AB and Reologica Instruments AB.

From them, I would like to thank Ene Pilman, for her support, and for bringing many tomato samples to the department! Bengt Jakobsson, for revealing many secrets about the potato fibres and bringing some samples every time I needed them. Mats Larsson, who came over many times to check the rheometer, and answered all my questions about it. And Anders Löfgren for shearing his experience about the rig with me. Many other people from these companies, for many meetings and shearing of ideas.

Also, Mats Bergsten, who provided the pump for the rig measurements when I badly needed it.

Many other people have contributed to this work in a more indirect way. My colleagues at the department, especially my roommate Hanna, who insisted I could speak Swedish and was very tolerant with my broken language, Carola for shearing the "writing a thesis period" with me, Tomas who help me with some math problems, Mattias helping me with some "tomato explosions" in the pilot plant, Margareta always knowing-how…mmmh well, I can not mention everyone, but all of you have contributed to create a friendly and nice atmosphere at the department!

My lunch-mates, Roberto, Ramiro, Federico, Christine, and some other people that join us from time to time, for these nice, relaxing breaks. Thanks also to all my friends for so many parties, and Sunday brunches, and dinners…, in short, thanks for your friendship and for making life so interesting! Maru, Mario, Laura, Eric, Jenny, Carol, Jamil and little Erik, Roberto, Lotta, Christine, Lucho, Anders, Krike, Ramiro, and Javi. I would also like to thank my friends in Barcelona, because no matter the time I have been away, I always feel like nothing has changed when I'm back there.

I would also like to thank my parents, Arturo y Rosa, for their unconditional support and love, despite they were not very sure what I was really doing in Sweden for such a long period of time… Gracias por estar siempre ahí, tan cerca, a pesar de la distancia.

Thanks, Giuliano, for being you, always.

References

Aguilera, J.M., 2005. Why food microstructure?. *Journal of Food Fngineering*, 67 (1-2), 3-11.

Annapragada, A., & Adjei, A., 1996. An analysis of the Fraunhofer diffraction method for particle size distribution analysis and its application to aerosolized sprays. *International Journal of Pharmaceutics*, 127 (2), 219-227.

Barnes H.A., & Nguyen, Q.D. 2001. Rotating vane rheometry – a review. *Journal of Non-Newtonian Fluid Mechanics*, 98 (1): 1-14.

Barnes, H.A., 1999. The yield stress – '*panta rei*' – everything flows? *Journal of Non-Newtonian Fluid Mechanics,* 81 (1-2): 133-178.

Barnes, H.A. 1997. Thixotropy –a review. *Journal of Non-Newtonian Fluid Mechanics,* 70, 1-33.

Barnes, HA, & Walters, K. 1985. The yield stress myth. *Rheologica Acta,* 24 (4): 323-326.

Bierwagen, G.P., & Saunders, T.E., 1974. Studies of effects of particle-size distribution on packing efficiency of particles. *Powder Technology*, 10 (3), 111-119.

Bistany K.L., & Kokini J.L. 1983. Comparison of steady shear rheological properties and small amplitude dynamic viscoelastic properties of fluid food materials. *Journal of Texture Studies* 14 (2): 113-124

Brouwers, H.J.H., 2006. Particle-size distribution and packing fraction of geometric random packing. *Physical Review E*, 74 (3), 031309.

Buscall, R., McGowan, I.J., Mills, P.D.A., Stewart, R.F., Sutton, D., White, L.R., & Yates, G.E., 1987. The rheology of strongly-flocculated suspensions. *Journal of Non-Newtonian Fluid Mechanics*, 24 (2), 183-202.

Buscall, R., Mills, P.D.A., Goodwin, J.W., & Lawson, D.W., 1988. Scaling behaviour of the rheology of aggregate networks formed from colloidal particles. *Journal of the Chemical Society-Faraday Transactions I*, 84, 4249-4260, Part 12.

Channell, G.M., Miller, & K.T., Zukoski, C.F., 2000. Effects of microstructure on the compressive yield stress. *AIChE Journal*, 46 (1), 72-78.

Cheng, D.C.H. 1986. Yield stress - a time-dependent property and how to measure it. *Rheologica Acta,* 25 (5): 542-554.

Chou, T.D., & Kokini, J.L. 1987. Rheological properties and conformation of tomato paste pectins, citrus and apple pectins. J*ournal of Food Science*, 52 (6): 1658-1664.

Citerne, G.P., Carreau, P.J. & Moan, M. 2001. Rheological properties of peanut butter. *Rheologica Acta*, 40, 86-96.

Coussot, P., & Ancey, A., 1999. Rheophysical classification of concentrated suspensions and granular pastes. *Physical Review E*, 59 (4), 4445-4457.

De Kee, D., Code, & R.K., Turcotte, G., 1983. Flow properties of time-dependent foodstuffs. *Journal of Rheology*, 27 (6), 581-604.

Den Ouden, F.W.C., & Van Vliet, T., 1997. Particle size distribution in tomato concentrate and effects on rheological properties. *Journal of Food Science*, 62 (3), 565-567.

Den Ouden, F.W.C., 1995. *Physico-chemical stability of tomato products*. Ph.D. Thesis, Wageningen Agricultural University.

Dervisoglu, M., & Kokini, J.L. 1986. Effect of different tube materials on the steady shear tube flow of semi-solid foods. *Journal of Food Process Engineering,* 8, 137-146.

Doraiswamy, D., Mujumdar, A.N., Tsao, I., Beris, A.N., Danforth, S.C. & Metzner, A.B. 1991. The Cox-Merz rule extended: a rheological model for concentrated suspensions and other materials with yield stress. *Journal of Rheology*, 35 (4), 647-685.

Dzuy, N.Q., & Boger, D.V. 1983. Yield stress measurement for concentrated suspensions. *Journal of Rheology,* 27 (4): 321-349.

Farris, R.J., 1968. Prediction of the viscosity of multimodal suspensions from unimodal viscosity data. *Transactions of the Society of Rheology*, 12 (2), 281-301.

Ferry, J.D., 1980. Viscoelastic properties of polymers (3rd ed.). New York: Wiley.

Fito, P.J., Clemente, G., & Sanz, F.J., 1983. Rheological behavior of tomato concentrate (hot break and cold break). *Journal of Food Engineering*, 2, 51-62.

Getchell, R.N., & Schlimme, D.V., 1985. Particle-size of water insoluble tomato solids measured by laser instrumentation. *Journal of Food Science*, 50 (5), 1495-1496.

Gleissle, W. & Hochstein, B. 2003. Validity of the Cox-Merz rule for concentrated suspensions. *Journal of Rheology*, 47 (4), 897-910.

Harper, J.C., & El Sahrigi, A.F., 1965. Viscometric behavior of tomato concentrates. *Journal of Food Science*, 30 (3), 470-475.

Hurtado, M.C., Greve, L.C., Labavitch, J.M. 2002. Changes in cell wall pectins accompanying tomato (*Lycopersicon esculentum* Mill.) paste manufacture. *Journal of Agriculture and Food Chemistry*, 50, 273-278.

Ilker, R., & Szczesniak, A.S., 1990. Structural and chemical bases for texture of plant foodstuffs. *Journal of Texture Studies*, 21 (1), 1-36.

Jeffery, BG.B. 1922. In: *The structure and Rheology of Complex Fluids*, ed. R.G. Larsson, 1999.

Kalyon, D.M. 2005. Apparent slip and viscoplasticity of concentrated suspensions. *Journal of Rheology,* 49 (3), 621-640.

Kokini, J.L., & Dervisoglu, M. 1990. Wall effects in the laminar pipe flow of four semi-solid foods. *Journal of Food Engineering,* 11, 29-42.

Krulis, M., & Rohm, H., 2004. Adaption of a vane tool for the viscosity determination of flavoured yoghurt. *European Food Research and Technology*, 218 (6), 598-601.

Larsson, R.G., 1999. *The Structure and Rheology of Complex Fluids.* New York: Oxford University Press.

Lee, D.I., 1970. Packing of spheres and its effect on viscosity of suspensions. *Journal of Paint Technology*, 42 (550), 579-587

Lee, Y., Bobroff, S. & McCarthy, K.L. 2002. Rheological characterization of tomato concentrates and the effect on uniformity of processing. *Chemical Engineering Communications,* 189 (3), 339-351.

Lin, H.J., Qin, X.M., Aizawa, K., Inakuma, T., Yamauchi, R. & Kato, K. 2005. Chemical properties of water-soluble pectins in hot- and cold-break tomato pastes. *Food Chemistry,* 93 (3), 409-415.

Liu, X., Qian, L., Shu, T., & Tong, Z., 2003. Rheology characterization of sol-gel transition in aqueous alginate solutions induced by calcium cations through in situ release. *Polymer*, 44, 407-412.

Macosko, C.W., 1994. *Rheology: Principles, Measurements And Applications.* New York: Wiley.

Marti, I., Höfler, O., Fischer, P. & Windhab, E.J. 2005. Rheology of concentrated suspensions containing mixtures of spheres and fibres. *Rheologica Acta,* 44, 502-512.

Martin, P.J. & Wilson, D.I. 2005. A critical assessment of the Jastrzebski interface condition for the capillary flow of pastes, foams and polymers. *Chemical Engineering Science*, 60, 493-502.

Mewis, J. 1979. Thixotropy – A general review. *Journal of non-Newtonian Fluid Mechanics,* 6, 1-20.

Miller, K.T., Melant, R.M., & Zukoski, C.F. 1996. Comparison of the compressive yield response of aggregated suspensions: Pressure filtration, centrifugation and osmotic consotidation. *Journal Of The American Ceramic Society,* 79 (10): 2545-2556.

Mills, P.D.A., Goodwin, J.W., & Grover, B.W., 1991. Shear field modification of strongly flocculated suspensions – aggregate morphology. *Colloid and Polymer Science*, 269 (9), 949.

Mooney, M. 1931. Explicit formulas for slip and fluidity. *Journal of Rheology*, 2 (2), 210-222.

Muliawan, E.B & Hatzikiriakos, S.G. 2007. Rheology of mozzarella cheese. *International Dairy Journal,* 17, 1063-1072.

Muthkumar, M. 1985. Dynamics of polymeric fractals. *Journal of Chemical Physics,* 83 (6), 3161-3168.

Nakajima, N., & Harrell, E.R., 2001. Rheology of PVC plastisol: particle size distribution and viscoelastic properties. *Journal of Colloid and Interface Science*, 238 (1), 105-115.

Narine, S.S., & Marangoni, A.G., 1999. Mechanical and structural model of fractal networks of fat crystals at low deformations. *Physical Review E*, 60 (6), 6991-7000.

Nguyen, Q.D., & Boger, D.V. 1992. Measuring the flow properties of yield stress fluids. *Annual Review of Fluid Mechanics* 24: 47-88.

Plucinski, J., Gupta, R.K. & Chakrabarti, S. 1998. Wall slip of mayonnaises in viscometers. *Rheologica Acta,* 37, 256-269.

Powers, S:R: & Somerford, D.J. 1978. Fibre sizing using Fraunhofer diffraction. *Optics Communications*, 26 (3), 313-317.

Qiu, C.G., & Rao, M.A. 1989. Effect of dispersed phase on the slip coefficient of apple sauce in a concentric cylinder viscometer. *Journal of Texture Studies,* 20 (1): 57-70.

Raeuber, H.J., & Nikolaus, H., 1980. Structure of foods. *Journal of Texture Studies*, 11 (3), 187-198.

Rao, M.A. & Cooley, H.J. 1992. Rheological behaviour of tomato pastes in steady and dynamic shear. *Journal of Texture Studies,* 23, 415-425.

Rao, M.A., 1999. *Rheology of Fluid and Semisolid Foods. Principles and Applications.* Maryland, Aspen Publishers, Inc.

Ross-Murphy, S.B., 1988. Small deformation measurements. In J.M.V. Blanshard, & J.R. Mitchell (Eds.), *Food Structure – its Creation and Evaluation* (pp. 387-400), London: Butterworths.

Russ, J.C. 2007. *The Image Processing Handbook.* Fifth edition, CRC, Boca Raton.

Servais, C., Jones, R., & Roberts, I., 2002. The influence of particle size distribution on the processing of food. *Journal of Food Engineering,* 51 (3), 201-208.

Shah, S.A., Chen, Y.-L., Schweizer, K.S., & Zukoski, C.F., 2003. Viscoelasticity and rheology of depletion flocculated gels and fluids. *Journal of Chemical Physics,* 119 (16), 8747-8760.

Steeneken, P.A.M., 1989. Rheological properties of aqueous suspensions of swollen starch granules. *Carbohydrate Polymers,* 11 (1), 23-42.

Steffe, J.F. 1996. *Rheological Methods In Food Process Engineering.* Second edition. Freeman Press, USA.

Thakur B.R., Singh R.K., & Nelson P.E. 1996. Quality attributes of processed tomato products: A review. *Food Reviews International,* 12 (3): 375-401.

Thakur, B.R., Singh, R.K., & Handa, A.K., 1995. Effect of homogenization pressure on consistency of tomato juice. *Journal of Food Quality,* 18 (5), 389-396.

Tiziani, S., & Vodovotz, Y., 2005. Rheological effects of soy protein addition to tomato juice. *Food Hydrocolloids,* 19 (1), 45-52.

Tornberg, E. 1978. Functional characterisation of protein stabilised emulsions: emulsifying behaviour of proteins in a valve homogeniser. *Journal of the Science of Food and Agriculture,* 29, 867-879.

Valencia, C., Sánchez, M.C., Ciruelos, A., & Gallegos, C., 2004. Influence of tomato paste processing on the linear viscoelasticity of tomato ketchup. *Food Science and Technology International,* 10 (2), 95-100.

Valencia, C., Sanchez, M.C., Ciruelos, A., Latorre, A., Madiedo, J.M., & Gallegos, C. 2003. Non-linear viscoelasticity modeling of tomato paste products. *Food Research International*, 36 (9-10): 911-919.

Whittle, M, & Dickinson, E. 1998. Large deformation rheological behaviour of a model particle gel. *Journal Of The Chemical Society-Faraday Transactions* 94 (16): 2453-2462.

Windhab, E. 1988. A new method for highly sensitive determination of the yield stress and flow behaviour of concentrated suspensions. In *Xth International Congress on Rheology*, Sydney, Australia.

Wyss, H.M., Deliormanli, A.M., Tervoort, E & Gauckler, L.J. 2005. Influence of microstructure on the rheological behaviour of dense particle gels. *AIChE Journal,* 51 (1), 134-141.

Wyss, H.M., Tervoort, E.V., & Gauckler, L.J., 2005. Mechanics and microstructures of concentrated particle gels. *Journal of the American Ceramic Society*, 88 (9), 2337-2348.

Xu, S.Y., Shoemaker, C.F., & Luh, B.S., 1986. Effect of break temperature on rheological properties and microstructure of tomato juices and pastes. *Journal of Food Science*, 51, 399.

Xu, S.Y., Shoemaker, C.F., & Luh, B.S., 1986. Effect of Break Temperature on Rheological Properties and Microstructure of Tomato Juices and Pastes. *Journal of Food Science*, 51 (2), 399.

Yeow, Y.L., Lee, H.L., Melvani, A.R. & Mifsud, G.C. 2003. A new method of processing capillary viscometry data in the presence of wall slip. *Journal of Rheology,* 47 (2), 337-348.

Yeow, Y.L., Nguyen, Y.T., Vu, T.D. & Wong, H.K. 2000. Processing the capillary viscometry data of fluids with yield stress. *Rheologica Acta*, 39, 392-398.

Yeow, Y.L., Perona, P., & Leong, Y.K. 2001. A reliable method of extracting the rheological properties of fruit purees from flow loop data. *Journal of Food Engineering,* 67 (4), 1407-1411.

Yilmazer U., & Kalyon D.M. 1989. Slip effects in capillary and parallel disk torsional flows of highly filled suspensions. *Journal of Rheology* 33 (8): 1197-1212.

Yoo, B., Rao, M.A., & Steffe, J.F., 1995. Yield stress of food dispersions with the vane method at controlled shear rate and shear-stress. *Journal of Texture Studies*, 26 (1), 1-10.